Transport and Fate Of Water and Chemicals in Laboratory Scale, Single Layer Aquifers

Volume 1. Mathematical Model

Special Report 845
September 1989

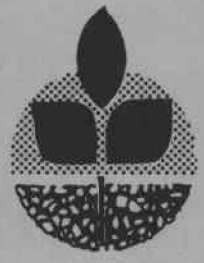

Agricultural Experiment Station
Oregon State University

Transport and Fate Of Water and Chemicals in Laboratory Scale, Single Layer Aquifers

Volume 1. Mathematical Model

F. T. Lindstrom
L. Boersma
M. A. Barlaz
F. Beck [1]

This is one of two volumes describing a mathematical model for the steady state flow field, transport, and fate of chemicals in laboratory scale, single layer aquifers.

[1]F. T. Lindstrom is Associate Professor and L. Boersma is Professor in the Department of Soil Science, Oregon State University, Corvallis, Oregon. M. A. Barlaz is a Post-Doctoral Fellow in the Department of Soil Science, OSU, stationed at the Robert S. Kerr Environmental Research Laboratory (RSKERL) of the U.S. Environmental Protection Agency at Ada, Oklahoma. F. Beck is a scientist at the RSKERL, USEPA at Ada, Oklahoma.

Foreword

Increasing awareness of groundwater enrichment with agricultural chemicals, specifically nitrates, herbicides and pesticides, has led to proposals for restoration of water quality. Many of the proposed strategies involve the use of microorganisms to transform harmful chemicals to a less harmful form. One such process is the removal of nitrates by denitrification. This is the microbially mediated process of converting NO_3 to the gases N_2O and/or N_2. After oxygen depletion the reduction of nitrate to nitrous oxide or elemental nitrogen is a metabolic process used by a wide variety of bacteria as an alternative to aerobic respiration. The proposed remediation strategy seeks to use existing populations of microorganisms for enhanced denitrification by injecting a carbon source into the aquifer. The technologies are being evaluated in laboratory scale models of aquifers. This report presents a mathematical model that describes the transport and fate processes in the laboratory models. The model provides a basis for extrapolation of laboratory findings. Further developments will add microbiological processes to the physical and chemical processes addressed in this report.

Acknowledgement

This publication reports results of studies supported by cooperative agreement number CR 814502–01–1, "Transport and Fate of Solutes in Unsaturated/Saturated Soils." This agreement is between the Robert S. Kerr Environmental Research Laboratory of the Environmental Protection Agency at Ada, Oklahoma, and Oregon State University, Corvallis, Oregon. The Oregon Agriculture Experiment Station provided facilities and additional support.

Contents

List of Figures

Transport and Fate of Water and Chemicals in Laboratory Scale, Single Layer Acquifers

Volume I. Mathematical Model

Abstract

A two-dimensional mathematical model for simulating the transport and fate of organic chemicals in a laboratory scale, single layer aquifer is presented. The aquifer is assumed to be homogeneous and isotropic with respect to its fluid flow properties. The physical model has open inlet and outlet ends and is bounded by impermeable walls on all sides with fully penetrating injection and/or extraction wells. The inlet and outlet ends have user-prescribed hydraulic pressure fields. The hydraulic pressure field, in the steady state, as a function of the space coordinates in the horizontal plane, is estimated first by using the classical two-dimensional Darcy flow law and the continuity equation, with the time partial derivatives being set to zero. The x and y components of the Darcy velocity are estimated by using Darcy's law. The chemical transport and fate equation is then solved in terms of user-stipulated initial and boundary conditions. The model accounts for the major physical processes of dispersion and advection, and also can account for linear equilibrium (Freundlich) sorption, five first–order loss processes, including microbial degradation, irreversible sorption and/or dissolution into the organic phase, radioactive decay, metabolism in the sorbed state, and radioactive decay in the sorbed state. The chemical may be released internally via distributed leaks, sources that do not perturb the flow field, or from fully penetrating injection wells. Chemical compound may also enter at the inlet boundary. Chemical mass balance type inlet and outlet boundary conditions are used. The solution to the field equation for hydraulic pressure is approximated by the classical space–centered finite difference method using a modified alternating direction, iterative implicit, procedure adapted from the classical Peaceman–Rachford concept. A solution to the transport and fate equation is approximated with a forward in time Euler–Lagrange time integrator applied to the chemical transport and fate semi–discretization.

Chapter 1

Introduction

Aquifer pollution is an emerging and rapidly growing problem in the United States (Pye et al. , 1983). Groundwater contamination is insidious because measurements of the problem have only recently been made on a consistent basis. As the data base increases, the pollution problem continues to increase.

Pollution can result from catastrophic events such as spills of toxic or otherwise hazardous compounds. Other important point sources include leaking storage facilities (Barcelona and Naymik, 1984; Thomas et al. , 1987) and waste product disposal (Canter and Knox, 1985). A growing concern in many areas is the effect of agricultural practices on groundwater quality (Fairchild, 1987). This form of contamination, generally described as nonpoint source pollution, is a cumulative effect both across a land area and in time. Nitrate contamination of groundwater is an example of agricultural pollution. The problem is increasing (Fairchild, 1987) and, partly because the source of pollutant is poorly defined, it is likely to continue to grow.

Methods to decrease aquifer nitrate levels include decreasing or eliminating the pollutant source (Canter and Knox, 1985; Fairchild, 1987). This approach is reasonable since loss of nitrate from agricultural systems constitutes an economic loss to producers. This quantitative factor and the more qualitative factor of decreasing environmental pollution have direct benefits to society. A second, more expensive method to improve groundwater quality is to remove the pollutant from the groundwater.

A variety of methods have been used to restore the quality of groundwater. The two major categories are physical containment and chemical and/or biological treatment (Lehr and Nielsen, 1982). Physical methods, including placement of barriers or hydrodynamic control by pumping, have been used with some success but are most effective when used to isolate point sources of pollution. Removal of the pollutant from the groundwater is a more reasonable strategy for pollutants contributed by nonpoint sources or by widely distributed sources. Chemical and biological methods are commonly used in situations where water is pumped out, treated, and used (e.g. van der Hoek and Klapwijk, 1987). This class of methods is used extensively for drinking water supplies where the end product is important enough to justify the expense.

A significant advantage of chemical and biological methods is the possibility of *in situ* aquifer restoration. A number of chemical techniques have been used *in situ* (Brown et al. , 1985) and there is considerable interest in the rapidly growing field of biorestoration (Alexander, 1980; Lehr and Nielsen, 1982; Brown et al. , 1985). The challenge of *in situ* methods is maintaining appropriate conditions in the aquifer itself. For biorestoration, the important factors affecting rate and efficiency of contaminant degradation are 1) presence of microbes suitable for degrading the pollutants; 2) energy sources and electron acceptors to sustain adequate microbial growth; 3) distribution of pollutant, substrate, and organisms in the aquifer; and 4) flow properties of the aquifer, including well locations and flow rates.

A number of studies have demonstrated that there is microbial activity in aquifers (Wilson et al. , 1983; Balkwill and Ghiorse, 1985; White et al. , 1985). Such organisms are generally considered to be substrate limited, particularly in anaerobic environments (Beeman and Suflita, 1987). In fact, pollutants have probably stimulated microbial activity by increasing substrate concentrations (Wilson et al. , 1983). Biological denitrification has been observed in aquifers (Lowrance, 1987) and in saturated sediments (Dodds and Jones, 1987). Findings from low-temperature environments indicate that denitrifiers can function under normal aquifer conditions. There are also limited data that suggest that carbon substrate additions may increase nitrate utilization (Obenhuber et al. , 1987).

Several studies provide evidence that biorestoration processes occur in aquifers. The evidence is clear for degradation of hydrocarbons in aerobic aquifer environments (Borden et al. , 1986; Brown et al. , 1985) where microbial counts, oxygen consumption, and hydrocarbon loss all increase. Denitrification has been observed in aquifers (Lowrance, 1987), artificial aquifers (Betz et al. , 1983), and in microcosms constructed of aquifer materials (Obenhuber et al., 1987). In addition, biological denitrification is commonly observed in reactors designed to treat groundwater after it has been pumped to a surface treatment site (van der Hoek and Klapwijk, 1987).

The experiments listed above indicate the potential for aquifer restoration by biological denitrification. The utility of biorestoration methods depends on establishing the proper conditions for microbial population growth. In addition, field-scale restoration depends on the distribution of microbes, substrate, and nitrate. The limiting factor among these is usually substrate concentration. Therefore, effective biorestoration methods require injection of a carbon source (Lehr and Nielsen, 1982; Brown et al. , 1985).

Aquifer injection and plume movement have been studied extensively, particularly using solute transport models. Naymik (1987) provides a good review of the literature and important issues. Models have been useful for developing an understanding of basic processes affecting solute distribution in aquifers but are generally not precise enough to predict field situations reliably (Naymik, 1987). Other reports are by Beccari et al. , 1983; Bodvarsson, 1984; Gorelick et al. , 1984; Kissel et al. , 1984.

The common failing of models for field situations is the treatment of dispersion (Devary and McKeon, 1986; Molz et al. , 1983; Pickens and Grisak, 1981; Smith and Schwartz, 1981). If inadequate data are available to characterize aquifer hydraulic conductivity, the dispersion coefficient must be increased to include the apparent dispersion caused by variation in aquifer material properties. This results in a scale-dependent dispersion coefficient based on the specific properties of the flow system under investigation rather than the

properties of the porous medium. Predictions of substrate spreading are only as good as the theoretical understanding and the field data that are available. This includes understanding dispersion and availability of hydraulic conductivity coefficients applicable to field situations. Understanding of the flow field at an aquifer restoration site is critical because methods for spreading added constituents through the aquifer depend on reliable prediction of the effects of injection rate and concentration, injection pulsing, and pumping from adjacent wells.

If biological denitrification is to be used as an effective technique for restoration, a fundamental understanding of the transport and fate processes is required. In addition, knowledge about the important limiting factors or limiting system properties must be acquired. Therefore, the immediate objective was to develop a conceptual model and computer code to describe substrate injection into an aquifer and to use the model in a sensitivity fashion to assess the magnitude of the physical and biological factors controlling aquifer denitrification processes and identify those which can be manipulated to enhance the process.

The mathematical model addresses aquifer fluid transport phenomena, including injection and withdrawal wells. Solute movement includes advection, dispersion, molecular diffusion and both chemical and biological reactions in the aquifer. The mathematical modeling effort presented here is part of an ongoing aquifer restoration study being conducted by the Environmental Protection Agency in cooperation with Oregon State University (R. S. Kerr Environmental Research Laboratory, of the USEPA, Ada, Oklahoma). One of the long-term goals of this study is development of a mathematical model of aquifer denitrification processes by stimulation of microbial populations.

Chapter 2

Statement of the Problem

Two large-scale (4 ft wide, 4 ft high, 16 ft long), three-layer physical aquifers were constructed at the USEPA Robert S. Kerr Environmental Research Laboratory in Ada, Oklahoma. These are to be used for experimental evaluation of proposed remediation scenarios (Fig. 2.1). These two aquifers, each containing three horizontal layers of material, with each layer assumed to be homogenous and isotropic with respect to water flow, can be used for validation of mathematical models that simulate hydrodynamic pressure distribution (Yates, 1988a,b), the transport and fate of chemicals, and evaluation of the growth characteristics of indigenous microbial populations. Basic transport, fate, growth, and decay process laws are used as building blocks for the mathematical model.

The mathematical model, reported here, is part of an evolutinary process in modeling, with the long-term goal of describing the transport and fate of chemicals in the full three-dimensional, laboratory-scale physical aquifers, described above. An immediate objective was to construct a two–dimensional, horizontal, water and chemical transport and fate model. The model was developed for a situation which consists of a single layer representing the aquifer portion of the three soil layers making up the RSKERL aquifers. Smaller–scale mathematical models based on the same fundamental physical, chemical, and biological process laws, believed to be operating in the larger aquifers, can and should also be tested or validated first against simpler laboratory–scale physical aquifers, composed of the same porous media. These smaller aquifers can be either destructively sampled or sampled repetitively in continuous time. The RSKERL models are made with homogeneous and isotropic soil slabs, have impermeable (no flow) side walls, and an impermeable bottom boundary. The top boundary is assumed to be a "no-flow" boundary also. Hydraulic heads at inlet and exit boundaries are prescribed. Injection and extraction wells are present. This model should make it possible to validate most of the large number of the individual transport and fate process laws, which will eventually be synthesized into the full three–dimensional model structure. The important features of this particular model are:

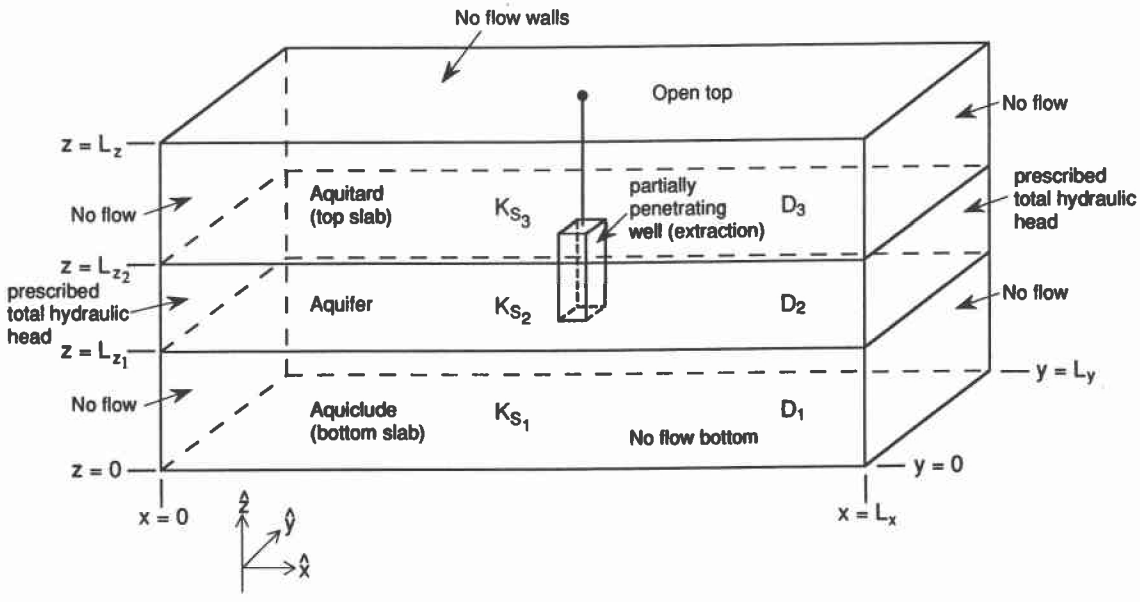

Figure 2.1: Schematic diagram of laboratory models used for the studies of acquifer restoration at Robert S. Kerr Environmental Research Laboratory.

1. Two-dimensional horizontal steady state fluid flow field defined by a hydraulic head field which is dependent upon appropriate Dirichlet and Neumann boundary conditions;

2. Two-dimensional transport and fate of chemicals in the aquifer. The distribution of chemicals is affected by:

   (a) advection and dispersion in longitudinal and transverse directions;

   (b) linear equilibrium (Freundlich) adsorption/desorption processes on each of the porous medium fractions;

   (c) five different first-order loss processes, including

      i. either metabolism by soil microbes or chemical reaction with other soil components in the free phase,

      ii. radioactive decay in the free phase,

      iii. other irreversible processes in the free phase,

      iv. either metabolism or chemical reaction in the sorbed phase, and

      v. radioactive decay in the sorbed phase;

   (d) the presence of zero order sources of chemical;

   (e) appropriate Dirichlet and Neumann boundary conditions with a provision for nonzero initial distribution of the chemical; and

   (f) the presence of fully penetrating injection and/or extraction wells.

A complete listing of the mathematical symbols, their meaning and units used in the model is given on the following pages.

Nomenclature and Notations Used for the Model

Fluid Flow Field

Symbol	*Description*	*Units*
$\mathbf{q}$	Darcy velocity vector	m/day
q_x	x-component of Darcy velocity	m/day
q_y	y-component of Darcy velocity	m/day
$\mathbf{U}$	average intervoid velocity	(m/day)
Ux	x-component of average intervoid velocity	(m/day)
Uy	y-component of average intervoid velocity	(m/day)
K_s	saturated hydraulic conductivity	(m/day)
H	hydraulic head field	(m water)
H_{in}	hydraulic head field at $y = 0$	(m water)
H_{out}	hydraulic head field at $y = Ly$	(m water)

Nomenclature and Notations Used for the Model
Fluid Flow Field

Symbol	*Description*	*Units*
x	transverse spatial component	(m)
y	longitudinal spatial component	(m)
ϵ	volume porosity of porous medium	(m^3/m^3)
ρ_w	density of water	(kg/m^3)
Q_{inj}	injection well mass density rate	$\left(\frac{kg\ \text{water}}{m^3\text{–day}}\right)$
Q_{out}	extraction well mass density rate	$\left(\frac{kg\ \text{water}}{m^3\text{–day}}\right)$
∇	"del" or nabla vector operator	$(1/m)$
L_x	transverse width of aquifer	(m)
L_y	longitudinal length of aquifer	(m)
∇^2	Laplace operator	$(1/m^2)$
$\mathcal{D}$	$\{(x,y)\ in\ R^2 \mid (0 < x < L_x) \times (0 < y < L_y)\}$	none
N_x	Number of subintervals into which the interval $[0,\ L_x]$ is partitioned. There are $N_x - 1$ internal nodes on the transverse coordinate and $N_x + 1$ total nodes along this same coordinate.	
N_y	Number of subintervals into which the interval $[0,\ L_x]$ is partitioned. There are $N_y - 1$ internal nodes on the transverse coordinate and $N_y + 1$ total nodes along this same coordinate.	
A	a real symmetric positive definite $(N_x - 1) \bullet (N_y - 1)$ by $(N_x - 1) \bullet (N_y - 1)$ array used for computing $\tilde{\mathbf{H}}$	$(1/m\text{–day})$
$\mathbf{b}$	vector of boundary data in the hydraulic head field	$(1/\text{day})$
α_{ij}	ij^{th} correction factor used for correcting the area estimate for adjacent injection and/or pumping wells	

Nomenclature and Notations Used for the Model
Chemical Transport and Fate Field

Symbol	*Description*	*Units*
D_{xx}	x-component of dispersion	(m^2/day)
D_{yy}	y-component of dispersion	(m^2/day)
D_{xy}	cross-component of dispersion	(m^2/day)
α_{tort}	tortuosity factor (0.67 usually)	(dimensionless)
D_{L_O}	free-solution molecular diffusion coefficient of compound	(m^2/day)
α_{dispx}	x-component of dispersivity	(m)
α_{dispy}	y-component of dispersivity	(m)
$\lvert U_x \rvert$	magnitude of x-component of velocity field	(m/day)
$\lvert U_y \rvert$	magnitude of y-component of velocity field	(m/day)
R	retention parameter	(dimensionless)
t	elapsed time in days from commencing injection and/or pumping of chemical field	$(days)$
λ_{met}	total first-order free-phase loss rate constant due to microbial action	(1/day)
λ_{irr}	total first-order free-phase loss rate constant of all irreversible loss processes, e.g. chemical reactions	(1/day)
λ_{rad}	total first-order free-phase loss rate constant for radioactive decay	(1/day)
λ^s_{met}	total first-order sorbed-phase loss rate constant of all microbial action	(1/day)
λ^s_{rad}	total first-order sorbed-phase loss rate constant for radioactive decay	(1/day)
$\%_{sand}$	decimal percent sand in porous medium	(dimensionless)
$\%_{silt}$	decimal percent silt in porous medium (includes clay fraction)	(dimensionless)
$\%_{org}$	decimal percent organics in porous medium	(dimensionless)
ρ_{sand}	average particle density of quartz sand	(kg/m^3)
ρ_{silt}	average particle density of silt (including clay)	(kg/m^3)
ρ_{org}	average particle density of organics	(kg/m^3)

Nomenclature and Notations Used for the Model
Chemical Transport and Fate Field

Symbol	*Description*	*Units*
K_{sand}	linear equilibrium Freundlich constant for sand	$(m^3/kg$ sand$)$
K_{silt}	linear equilibrium Freundlich constant for silt	$(m^3/kg$ silt$)$
K_{org}	linear equilibrium Freundlich constant for organics	$(m^3/kg$ organics$)$
C	free-phase chemical concentration distribution (field)	(kg/m^3)
$\mathcal{S}$	linear equilibrium sorbed-phase chemical concentration distribution (field)	(kg/m^3)
Q_{so}	chemical source rate density for buried sources	$\left(\frac{kg\ \text{chem}}{m^3-\text{day}}\right)$
C_{in}	chemical concentration in inlet end mixing tank	(kg/m^3)
C_{out}	chemical concentration in outlet end mixing tank	(kg/m^3)
C_s	injection well chemical concentration	$\left(\frac{kg\,\text{chem}}{kg\,\text{solution}}\right)$
δt	time increment $t_{n+1} = t_n + \delta t$	(days)
$D_{c_{in}}$	average dispersion coefficient in the inlet tank	(m^2/day)
$D_{c_{out}}$	average dispersion coefficient in the outlet tank	(m^2/day)
$L_{y_{in}}$	longitudinal axis distance from the plane $y = 0$ to the center of the inlet-end mixing tank	(m)
$L_{y_{out}}$	longitudinal axis distance from the plane $y = L_y$ to the center of the exit-end mixing tank	(m)
V_{in}	inlet tank average axial velocity	(m/day)
V_{out}	exit tank average axial velocity	(m/day)
L_w	vertical thickness of the aquifer	(m)
L_{in}	length of the inlet end mixing tank	(m)
L_{out}	length of the exit end mixing tank	(m)
L_x	transverse coordinate width of aquifer	(m)
L_y	longitudinal coordinate length of aquifer	(m)

Chapter 3

Fluid Flow Field

3.1 Statement of the Problem

Figure 3.1 shows a schematic diagram of the smaller single layer aquifer physical model in the RSKERL laboratory. Water flows into and out from the soil via open ends and can be extracted or injected through fully penetrating injection and/or extraction wells. The transverse coordinate is x (meters) and the longitudinal coordinate is y (meters). The third coordinate z (meters) measures aquifer thickness. The porous medium is homogeneous and isotropic and has impervious walls on the sides and bottom. The upper boundary is assumed to be a zero flux boundary as well. These conditions allow evaluation of two-dimensional transport and fate.

The assumptions concerning the fluid flow field are:

1. The fluid flow field operates at steady state conditions at all times;
2. Any fluid flow perturbations introduced at either of the flow boundaries propagate extremely rapidly throughout the flow field, thus a new steady state is achieved rapidly and the fluid storativity term in the fluid flow model may be neglected (Bodvarsson, 1984);
3. The aquifer material is homogeneous and isotropic;
4. Dirichlet boundary conditions hold at both the inlet and outlet ends; $H_{in}\ (m)$ and $H_{out}\ (m)$, respectively, are specified and assumed to extend across, $0 \leq x \leq L_x$;
5. Neumann or flux type boundary conditions are specified along the walls, i.e. the $x = 0$ and $x = L_x$ planes;
6. The Darcy fluid velocity field components of the flow vector $\mathbf{q}\ (m/day)$ are defined by

$$\mathbf{q} = (\epsilon\, U_x,\ \epsilon\, U_y) = \left(-K_s\, \frac{\partial H}{\partial x},\ -K_s\, \frac{\partial H}{\partial y}\right) \tag{3.1}$$

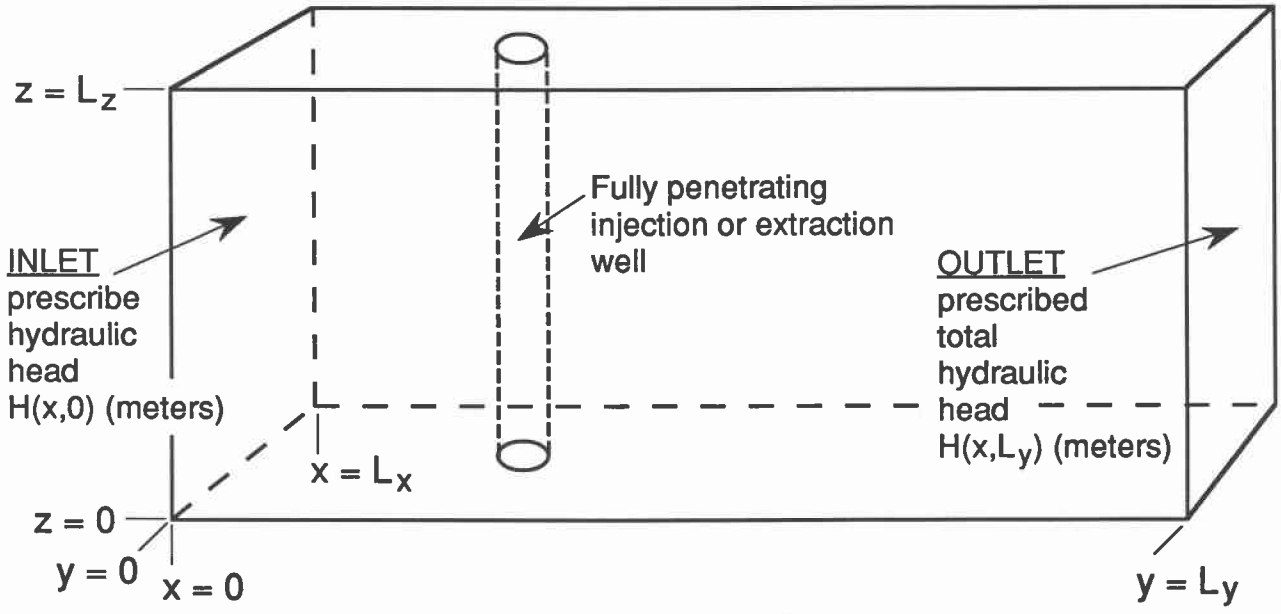

Figure 3.1: Schematic diagram of the physical model used for preliminary studies of transport and fate problems. The mathematical model is based on the physical structure shown here.

where K_s is the saturated hydraulic conductivity (m/day) in the aquifer and H is the hydraulic head (m).

Combining equation (3.1) with the steady state continuity equation for a representative elementary volume (REV) in the aquifer obtains

$$\nabla \bullet (\rho_w \, \epsilon \, \mathbf{U}) = (Q_{inj} - Q_{out}) \tag{3.2}$$

where ρ_w is the density of water (kg/m^3), Q_{inj} is the fluid mass injection rate $(kg/m^3 - day)$, and Q_{out} is the fluid mass extraction rate $(kg/m^3 - day)$.

Substitution for **U** in equation (3.2) leads to the well known Poisson problem in potential field theory:

$$\rho_w \left(\frac{\partial \left(-K_s \frac{\partial H}{\partial x} \right)}{\partial x} + \frac{\partial \left(-K_s \frac{\partial H}{\partial y} \right)}{\partial y} \right) = \rho_w \left(\frac{\partial (\epsilon \, U_x)}{\partial x} + \frac{\partial (\epsilon \, U_y)}{\partial y} \right)$$
$$= +(Q_{inj} - Q_{out}) \, , \tag{3.3}$$

where ϵ is the volumetric or area pore space $(m^3 \; voids/m^3 \; soil)$.

Boundary conditions, to be satisfied at all times, are written according to assumptions 4 and 5 as follows:

1. along $y = 0$ (inlet end),

$$H(x,0) = H_{in}(x),\ 0 \le x \le L_x\ , \tag{3.4}$$

2. along $y = L_y$ (outlet end),

$$H(x,L_y) = H_{out}(x),\ 0 \le x \le L_x\ , \tag{3.5}$$

3. along $x = 0$,

$$\frac{\partial H}{\partial x} = 0\ , \tag{3.6}$$

4. along $x = L_x$,

$$\frac{\partial H}{\partial x} = 0\ . \tag{3.7}$$

As K_s is a constant for the physical model, equation (3.3) simplifies to

$$\frac{\partial^2 H}{\partial x^2} + \frac{\partial^2 H}{\partial y^2} = -\frac{(Q_{inj} - Q_{out})}{\rho_w\, K_s} \tag{3.8}$$

on $(0 < x < L_x) \times (0 < y < L_y)$.

The unique solution of equation (3.8) subject to the above stated boundary conditions is

$$\begin{aligned} H(x,y) &= H_{in} + \left(\frac{H_{out} - H_{in}}{L_y}\right) y \\ &+ \sum_{n=0}^{\infty} \sum_{m=1}^{\infty} \beta_{nm} \cos\left(\frac{n\pi x}{L_x}\right) \sin\left(\frac{m\pi y}{L_y}\right)\ , \end{aligned} \tag{3.9}$$

where

$$\beta_{om} = \frac{L_y^2\, \alpha_{om}}{K_s\, \rho_w\, \pi^2\, m^2}\ , \qquad m = 1,2,3\ldots \tag{3.10}$$

$$\beta_{nm} = \frac{\alpha_{nm}}{K_s \rho_w \left(\frac{m^2\,\pi^2}{L_y^2} + \frac{n^2\,\pi^2}{L_x^2}\right)}\ , \qquad n = 1,2,3\ldots,\ m = 1,2,3\ldots \tag{3.11}$$

and

$$\begin{aligned} \alpha_{om} &= \frac{2}{L_y\, L_x} \int_0^{L_x} \int_0^{L_y} (Q_{inj}(\zeta,\eta) - Q_{out}(\zeta,\eta)) \\ &\sin\left(\frac{m\pi\eta}{L_y}\right) d\eta d\zeta\ , \qquad m = 1,2,3\ldots \end{aligned} \tag{3.12}$$

$$\alpha_{nm} = \frac{4}{L_y L_x} \int_0^{L_x} \int_0^{L_y} (Q_{inj}(\zeta,\eta) - Q_{out}(\zeta,\eta)) \sin\left(\frac{m\pi\eta}{L_y}\right) \cos\left(\frac{n\pi\zeta}{L_x}\right) d\eta d\zeta \,. \tag{3.13}$$

Equation (3.1) yields the Darcian velocity components

$$q_x = (\epsilon U_x) = -K_s \frac{\partial H}{\partial x} = +K_s \sum_{n=0}^{\infty} \sum_{m=1}^{\infty} \left(\frac{n\pi}{L_x}\right) \beta_{nm} \sin\left(\frac{n\pi x}{L_x}\right) \sin\left(\frac{m\pi y}{L_y}\right) , \tag{3.14}$$

$$q_y = (\epsilon U_y) = -K_s \frac{\partial H}{\partial y} = +K_s \left(\frac{H_{in} - H_{out}}{L_y}\right) - K_s \sum_{n=0}^{\infty} \sum_{m=1}^{\infty} \left(\frac{m\pi}{L_y}\right) \beta_{nm} \cos\left(\frac{n\pi x}{L_x}\right) \cos\left(\frac{m\pi y}{L_y}\right) . \tag{3.15}$$

These components are needed in the chemical transport and fate equation. It is possible to show, for a broad range of bounded and measurable Q_{inj} and Q_{out} functions, that solutions to equations (3.14) and (3.15) exist, i.e. the double sums converge. However, the solutions are usually very slow to convergence. Thousands, if not millions, of terms are necessary to achieve the required number of significant digits in each velocity component. Thus, the hydraulic head field on $\mathcal{D}$, the interior of the long thin box, can be approximated via finite–difference, space centered methods.

3.2 Approximation to the Fluid Flow Equations

Figure 3.2 shows a local region of $\mathcal{D}$ on which a lattice of nodal points has been superimposed. $\mathcal{D}$ is the set of all $(x,y) \epsilon R^2$ such that $\{[0 < x < L_x] \times [0 < y < L_y]\}$, with nonhomogeneous nodal spacing in both coordinates.

Integrate both sides of equation (3.3) over the rectangular subregion $\mathcal{D}_{ij}$ where

$$\mathcal{D}_{ij} = \left\{(x,y) \text{ in } R^2 |\, x \text{ in } \left[x_{i-1} + \frac{\Delta x_{i-1}}{2},\, x_i + \frac{\Delta x_i}{2}\right] \text{ and } y \text{ in } \left[y_{j-1} + \frac{\Delta y_{j-1}}{2},\, y_j + \frac{\Delta y_j}{2}\right]\right\} . \tag{3.16}$$

For notational purposes define the points $y_{j-1/2} = y_{j-1} + \Delta y_{j-1}/2$, $y_{j+1/2} = y_j + \Delta y_j/2$, and so forth, and similarly for the x coordinate so that,

$$\int_{y_{j-1/2}}^{y_{j+1/2}} \int_{x_{i-1/2}}^{x_{i+1/2}} K_s \left(\frac{\partial^2 H}{\partial x^2} + \frac{\partial^2 H}{\partial y^2}\right) dx dy = -\rho_w \int_{\mathcal{D}ij} \int (Q_{inj} - Q_{out}) dx dy \,. \tag{3.17}$$

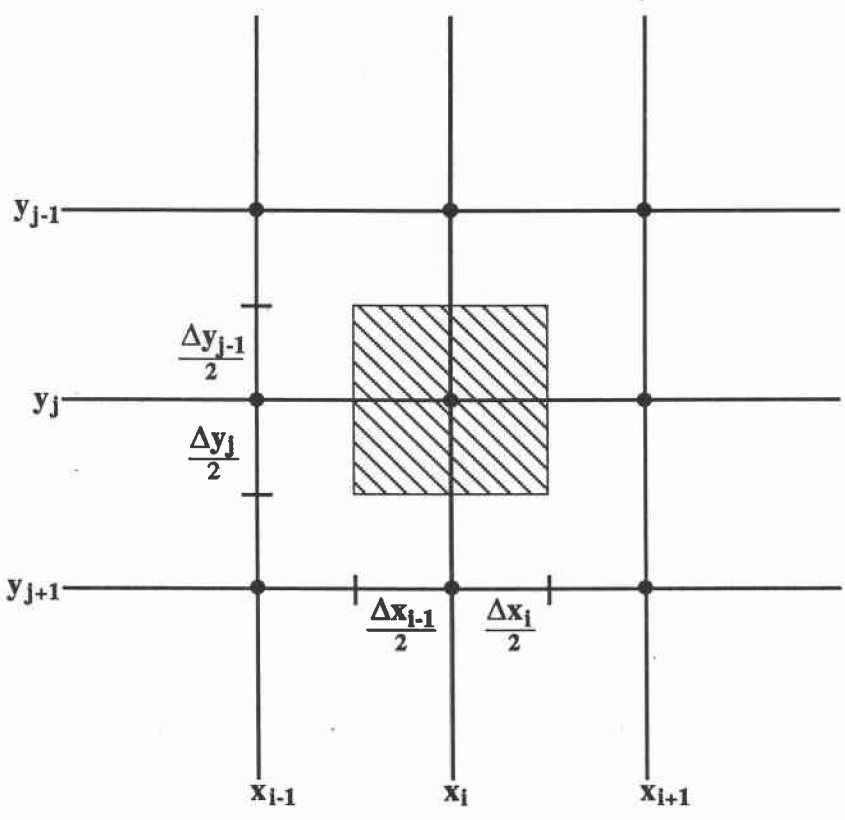

Figure 3.2: Local interior region of lattice points showing subregion $\mathcal{D}_{ij}$.

Carrying out the indicated integrations yields

$$\begin{aligned}\int_{y_{j-1/2}}^{y_{j+1/2}} & \left(K_s \left.\frac{\partial H}{\partial x}\right|_{x_{i+1/2}} - K_s \left.\frac{\partial H}{\partial x}\right|_{x_{i-1/2}} \right) dy \\ & + \int_{x_{i-1/2}}^{x_{i+1/2}} \left(K_s \left.\frac{\partial H}{\partial y}\right|_{y_{j+1/2}} - K_s \left.\frac{\partial H}{\partial x}\right|_{y_{j-1/2}} \right) dx \\ & = -\rho_w \int_{\mathcal{D}ij} \int (Q_{inj} - Q_{out}) dx dy \ . \end{aligned} \tag{3.18}$$

Approximating the four indicated partial derivatives via the 2nd order correct approximations,

$$\left.\frac{\partial H}{\partial x}\right|_{x_{i+1/2}} = \frac{H_{i+1}(y) - H_i(y)}{\Delta x_i} + O_1(\Delta x_i^2) \tag{3.19}$$

$$\left.\frac{\partial H}{\partial x}\right|_{x_{i-1/2}} = \frac{H_i(y) - H_{i-1}(y)}{\Delta x_{i-1}} + O_2(\Delta x_{i-1}^2) \tag{3.20}$$

$$\left.\frac{\partial H}{\partial y}\right|_{y_{j+1/2}} = \frac{H_{j+i}(x) - H_j(x)}{\Delta y_j} + O_3(\Delta y_j^2) \tag{3.21}$$

$$\left.\frac{\partial H}{\partial y}\right|_{y_{j-1/2}} = \frac{H_j(x) - H_{j-1}(x)}{\Delta y_{j-1}} + O_4(\Delta y_{j-1}^2) \ , \tag{3.22}$$

gives

$$\begin{aligned}\int_{y_{j-1/2}}^{y_{j+1/2}} & \left(K_s \left(\frac{H_{i+1} - H_i}{\Delta x_i} \right) - K_s \left(\frac{H_i - H_{i-1}}{\Delta x_{i-1}} \right) \right) dy \\ & + \int_{x_{i-1/2}}^{x_{i+1/2}} \left(K_s \left(\frac{H_{j+1} - H_j}{\Delta y_j} \right) - K_s \left(\frac{H_j - H_{j-1}}{\Delta y_{j-1}} \right) \right) dx \\ & = -O_5(\Delta x_i^2, \Delta x_{i-1}^2, \Delta y_j^2, \Delta y_{j-1}^2) \bullet \text{Length } (\mathcal{D}_{ij}) \\ & - \int_{\mathcal{D}_{ij}} \int \left(\frac{Q_{inj} - Q_{out}}{\rho_w} \right) dx dy \ , \end{aligned} \tag{3.23}$$

where length $(\mathcal{D}_{ij})$ is the length of the positive oriented arc circumscribing the subregion $\mathcal{D}_{ij}$.

Next, it is supposed that

$$\frac{H_{i+1}(y) - H_i(y)}{\Delta x_i}$$

is held fixed at its respective value at $y = y_j$. In like fashion the other three line integrals are then treated so that upon dropping the error terms and defining $\tilde{H}_{i,j}$ to be the approximate hydraulic pressure at nodal point (x_i, y_j) in $\mathcal{D}_{ij}$ obtains,

$$\left\{K_s\left(\frac{\tilde{H}_{i+1,j}-\tilde{H}_{i,j}}{\Delta x_i}\right)-K_s\left(\frac{\tilde{H}_{i,j}-\tilde{H}_{i-1,j}}{\Delta x_{i-1}}\right)\right\}\cdot \left(\frac{\Delta y_{j-1}+\Delta y_j}{2}\right)+\left\{K_s\left(\frac{\tilde{H}_{i,j+1}-\tilde{H}_{i,j}}{\Delta y_j}\right) - K_s\left(\frac{\tilde{H}_{i,j}-\tilde{H}_{i-1,j}}{\Delta y_{j-1}}\right)\right\}\cdot\left(\frac{\Delta x_{i-1}+\Delta x_i}{2}\right) = -A_{rea}(\mathcal{D}_{ij})\,\epsilon\,(Q_{inj}-Q_{out})_{ij}/\rho_w\,. \tag{3.24}$$

Multiplication of both sides by the reciprocal of the area of $\mathcal{D}_{ij}$,

$$\left(\frac{\Delta x_{i-1}+\Delta x_i}{2}\right)\left(\frac{\Delta y_{j-1}+\Delta y_j}{2}\right),$$

gives the "finite difference" form

$$\frac{K_s\left(\frac{\tilde{H}_{i+1,j}-\tilde{H}_{i,j}}{\Delta x_i}\right)-K_s\left(\frac{\tilde{H}_{i,j}-\tilde{H}_{i-1,j}}{\Delta x_{i-1}}\right)}{\left(\frac{\Delta x_{i-1}+\Delta x_i}{2}\right)} + \frac{K_s\left(\frac{\tilde{H}_{i,j+1}-\tilde{H}_{i,j}}{\Delta y_j}\right)-K_s\left(\frac{\tilde{H}_{i,j}-\tilde{H}_{i,j-1}}{\Delta y_{j-1}}\right)}{\left(\frac{\Delta y_{j-1}+\Delta y_j}{2}\right)} = -\left(\frac{Q_{inj}-Q_{out}}{\rho_w}\right)_{ij}. \tag{3.25}$$

In anticipation of the use of the classical alternating direction iterative implicit method (ADII method) of Peaceman and Rachford (Ch. 7, Varga, 1962), define the matrix elements as follows:

$$alt2_{i,j} = -\frac{K_s/\Delta x_{i-1}}{\left(\frac{\Delta x_{i-1}+\Delta x_i}{2}\right)}, \tag{3.26}$$

$$adtl_{i,j} = -\frac{K_s/\Delta x_{j-1}}{\left(\frac{\Delta y_{j-1}+\Delta y_j}{2}\right)}, \tag{3.27}$$

$$adt2y_{ij} = \frac{K_s/\Delta y_j + K_s/\Delta y_{j-1}}{\left(\frac{\Delta y_{j-1}+\Delta y_j}{2}\right)}, \tag{3.28}$$

$$adt2x_{ij} = \frac{K_s/\Delta x_i + K_s/\Delta x_{i-1}}{\left(\frac{\Delta x_{i-1}+\Delta x_i}{2}\right)}, \tag{3.29}$$

$$adt3_{i,j} = -\frac{K_s/\Delta y_j}{\left(\frac{\Delta y_{j-1}+\Delta y_j}{2}\right)}\,, \tag{3.30}$$

$$aut2_{i,j} = -\frac{K_s/\Delta x_i}{\left(\frac{\Delta x_{i-1}+\Delta x_i}{2}\right)}\,. \tag{3.31}$$

The coupled linear system of equations then results, for $i = 1,2,\ldots N_x - 1$, $j = 1,2,\ldots N_y - 1$,

$$\begin{aligned} &alt2_{i,j}\,\tilde{H}_{i-1,j} + adtl_{i,j}\,\tilde{H}_{i,j-1} \\ &\quad + (adt2x_{i,j} + adt2y_{ij})\,\tilde{H}_{i,j} + adt3_{i,j}\,\tilde{H}_{i,j+1} \\ &\quad + aut2_{i,j}\,\tilde{H}_{i+1,j} = -\left(\frac{Q_{inj} - Q_{out}}{\rho_w}\right)_{ij}\,. \end{aligned} \tag{3.32}$$

3.3 Boundary Conditions

Equations (3.4) and (3.5) are referred to as Dirichlet conditions because the total hydraulic field along the planes $y = 0$ and $y = L_y$ is specified. Hence,

$$H(x,o) = H_{in}(x_i) = \tilde{H}(x_i,o), \qquad 0 \le x \le L_x\,. \tag{3.33}$$

Similarly at $y = L_y$ define

$$\tilde{H}_{i,Ny} = H_{out}(x_i), \qquad 0 \le x \le L_x\,. \tag{3.34}$$

Equations (3.6) and (3.7) are referred to as Neumann conditions since the flux in the direction normal to the surface is specified. In this case, impermeable walls along the planes $x = 0$ and $x = L_x$ exist, so that a zero or no flux boundary condition obtains. That is, along $x = 0$, where $\partial H/\partial x = 0$, approximate for $j = 1,2,\ N_y - 1$,

$$\begin{aligned} \left.\frac{\partial H}{\partial x}\right|_{x=0} = 0 \doteq \Bigg\{ &-\left(2 + \frac{\Delta x_2}{\Delta x_1}\right)\tilde{H}_{o,j} + \left(\frac{\Delta x_2}{\Delta x_1} + 2 + \frac{\Delta x_1}{\Delta x_2}\right)\tilde{H}_{1,j} \\ &- \frac{\Delta x_1}{\Delta x_2}\,\tilde{H}_{2,j}\Bigg\} \,/\, (\Delta x_1 + \Delta x_2)\,, \end{aligned} \tag{3.35}$$

a formula obtained by differentiating the Lagrange, degree 2 interpolating polynomial,

$$\begin{aligned} P_2(x) \;=\; &\tilde{H}_{o,j} + \left(\frac{\tilde{H}_{1,j} - \tilde{H}_{o,j}}{\Delta x_1}\right)(x - x_o) \\ &+ \left(\frac{\frac{\tilde{H}_{2,j}-\tilde{H}_{1,j}}{\Delta x_2} - \frac{\tilde{H}_{1,j}-\tilde{H}_{o,j}}{\Delta x_1}}{\Delta x_1 + \Delta x_2}\right)(x - x_o)\,(x - x_o - \Delta x_1)\,, \end{aligned} \tag{3.36}$$

setting $x = x_o\,(= 0)$ with $P_2'(x_o) = 0$, and simplifying the result. Since Δx_1 and Δx_2 are positive, possibly nonuniform, nodal spacings the definition of $H_{o,j}$ is obtained as a linear combination of $H_{1,j}$ and $H_{2,j}$;

$$\tilde{H}_{o,j} = \frac{\left(2 + \frac{\Delta x_2}{\Delta x_1} + \frac{\Delta x_1}{\Delta x_2}\right) \tilde{H}_{1,j} - \frac{\Delta x_1}{\Delta x_2} \tilde{H}_{2,j}}{2 + \frac{\Delta x_2}{\Delta x_1}} . \tag{3.37}$$

It can be shown in like fashion that at $x = L_x$ where

$$\left.\frac{\partial H}{\partial x}\right|_{x=L_x} = 0 ,$$

$$\tilde{H}_{Nx,j} = \frac{\frac{-\Delta x_{Nx}}{\Delta x_{Nx-1}} \tilde{H}_{Nx-2,j} + \left(2 + \frac{\Delta x_{Nx}}{\Delta x_{Nx-1}} + \frac{\Delta x_{Nx-1}}{\Delta x_{Nx}}\right) \tilde{H}_{Nx-1,j}}{2 + \frac{\Delta x_{Nx-1}}{\Delta x_{Nx}}} , \tag{3.38}$$

for $j = 1, 2, \ldots N_y - 1$.

A standard Taylor series based error analysis leads to the errors:

- at $x = 0$,

$$0_1(\Delta x_1\ \Delta x_2) , \tag{3.39}$$

which if $\Delta x_1 = \Delta x_2 = \Delta x$ is $0_1(\Delta x^2)$; and

- at $x = L_x$,

$$0_2(\Delta x_{Nx}\ \Delta x_{Nx-1}) , \tag{3.40}$$

which if $\Delta x_{Nx} = \Delta x_{Nx-1} = \Delta x$ is $0_2(\Delta x^2)$.

It is good practice to choose Δx_1, Δx_2, Δx_{Nx-1}, Δx_{Nx} equal to about 1/10 the intradomain lattice node spacing.

3.4 Solution of the Linear System of Equations

A "vertical" or "horizontal" ordering of the nodes may be chosen in equation 3.32. In either case, when using the boundary data, as indicated, the system may be written in matrix form

$$A\tilde{\mathbf{H}} = \mathbf{b} , \tag{3.41}$$

where A is a real, possibly symmetric, $N_x - 1 \bullet N_y - 1$ by $N_x - 1 \bullet N_y - 1$, 5-band array, which is irreducible, weakly diagonally dominant, and positive definite, an M–array in the sense of Varga (1962, pp. 186-188), and $\mathbf{b}$ is the vector of boundary data. $\tilde{\mathbf{H}}$ then exists uniquely as

$$\tilde{\mathbf{H}} = A^{-1}\,\mathbf{b}\,. \tag{3.42}$$

Here we find $\tilde{\mathbf{H}}$ via the classical Peaceman-Rachford ADII method which involves alternating between x and y directions (Varga, 1962).

3.5 Velocity Components

Once all components of $\tilde{\mathbf{H}}$ are known, the x and y components of the fluid velocity field, namely the pore velocities, can be computed using equation (3.1). However, since the hydraulic head field $H(x,y)$ is known only approximately and only on a finite set of grid points, the two velocity components must be numerically estimated at each (x_i, y_j).

Two 3–point Lagrange polynomials, one in x and the other in y, similar to those stated in equation (3.36), are differentiated at the intranode points. Differentiation is done first along the x–coordinate to provide an estimate of $\partial H/\partial x|_{i,j}$ and secondly along the y–coordinate to provide an estimate of $\partial H/\partial y|_{i,j}$. For those nodes inside $\mathcal{D}$ and adjacent to the impervious walls as well as those nodes inside $\mathcal{D}$ but adjacent to the inlet and outlet boundaries, simple, 2–point–based velocity estimates are used. The formulas used are:

- at $y = 0$, for $i = 1, 2, \ldots N_x - 1$,

$$\left.\frac{\partial H}{\partial y}\right|_{y=0} \doteq \frac{\tilde{H}_{i,1} - \tilde{H}_{i,0}}{\Delta y_1}\,, \tag{3.43}$$

$$\begin{aligned}\left.\frac{\partial H}{\partial x}\right|_{y=0} \doteq & -\frac{\Delta x_i}{\Delta x_{i-1}(\Delta x_{i-1} + \Delta x_i)}\,\tilde{H}_{i-1,0} \\ & + \left(\frac{1}{\Delta x_{i-1}} - \frac{1}{\Delta x_i}\right)\tilde{H}_{i,0} \\ & + \frac{\Delta x_{i-1}}{\Delta x_i(\Delta x_{i-1} + \Delta x_i)}\,\tilde{H}_{i+1,0}\,,\end{aligned} \tag{3.44}$$

- at $y = L_y$, for $i = 1, 2, \ldots N_x - 1$,

$$\left.\frac{\partial H}{\partial y}\right|_{y=L_y} \doteq \frac{\tilde{H}_{i,Ny} - \tilde{H}_{i,Ny-1}}{\Delta y_{Ny}}\,, \tag{3.45}$$

$$\begin{aligned}\left.\frac{\partial H}{\partial x}\right|_{y=L_y} \doteq & -\frac{\Delta x_i}{\Delta x_{i-1}(\Delta x_{i-1} + \Delta x_i)}\,\tilde{H}_{i-1,Ny} \\ & + \left(\frac{1}{\Delta x_{i-1}} - \frac{1}{\Delta x_i}\right)\tilde{H}_{i,Ny} \\ & + \frac{\Delta x_{i-1}}{\Delta x_i(\Delta x_{i-1} + \Delta x_i)}\,\tilde{H}_{i+1,Ny}\,,\end{aligned} \tag{3.46}$$

- at $x = 0$, for $j = 1, 2, \ldots N_y - 1$,

$$\left.\frac{\partial H}{\partial x}\right|_{x=0} = 0 \text{ according to equation (3.6)}, \tag{3.47}$$

$$\begin{aligned}\left.\frac{\partial H}{\partial y}\right|_{x=0} \doteq & -\frac{\Delta y_i}{\Delta y_{j-1}(\Delta y_{j-1} + \Delta y_j)} \tilde{H}_{0,j-1} \\ & + \left(\frac{1}{\Delta y_{j-1}} - \frac{1}{\Delta y_j}\right) \tilde{H}_{0,j} \\ & + \frac{\Delta y_{j-1}}{\Delta y_j(\Delta y_{j-1} + \Delta y_j)} \tilde{H}_{0,j+1}\ ,\end{aligned} \tag{3.48}$$

- at $x = L_x$, for $j = 1, 2, \ldots N_y - 1$,

$$\left.\frac{\partial H}{\partial x}\right|_{x=L_x} = 0 \text{ according to equation (3.7)}, \tag{3.49}$$

$$\begin{aligned}\left.\frac{\partial H}{\partial y}\right|_{x=L_x} \doteq & -\frac{\Delta y_j}{\Delta y_{j-1}(\Delta y_{j-1} + \Delta y_j)} \tilde{H}_{Nx,j-1} \\ & + \left(\frac{1}{\Delta y_{j-1}} - \frac{1}{\Delta y_j}\right) \tilde{H}_{Nx,j} \\ & + \frac{\Delta y_{j-1}}{\Delta y_j(\Delta y_{j-1} + \Delta y_j)} \tilde{H}_{Nx,j+1}\ .\end{aligned} \tag{3.50}$$

For the remainder of the internal nodes write:

$$\begin{aligned}\left.\frac{\partial H}{\partial x}\right|_{x_i,y_j} \doteq & -\frac{\Delta x_i}{\Delta x_{i-1}(\Delta x_{i-1} + \Delta x_i)} \tilde{H}_{i-1,j} \\ & + \left(\frac{1}{\Delta x_{i-1}} - \frac{1}{\Delta x_i}\right) \tilde{H}_{i,j} \\ & + \frac{\Delta x_{i-1}}{\Delta x_i(\Delta x_{i-1} + \Delta x_i)} \tilde{H}_{i+1,j}\ ,\end{aligned} \tag{3.51}$$

and

$$\begin{aligned}\left.\frac{\partial H}{\partial y}\right|_{x_i,y_j} \doteq & -\frac{\Delta y_j}{\Delta y_{j-1}(\Delta y_{j-1} + \Delta y_j)} \tilde{H}_{i,j-1} \\ & + \left(\frac{1}{\Delta y_{j-1}} - \frac{1}{\Delta y_j}\right) \tilde{H}_{i,j} \\ & + \frac{\Delta y_{j-1}}{\Delta y_j(\Delta y_{j-1} + \Delta y_j)} \tilde{H}_{i,j+1}\ .\end{aligned} \tag{3.52}$$

With the exception of the formulas approximating $\partial H/\partial y$ along the open portions at $y = 0$ and $y = L_y$, which are $0(\Delta y)$ correct, the remaining approximations are $0(\Delta x_i\ \Delta x_{i-1})$ and $0(\Delta y_j\ \Delta y_{j-1})$ correct. These results are easily confirmed by means of standard Taylor series analysis. In preliminary work it has been found experimentally that to obtain U_x and U_y to three or four significant digits, $\tilde{H}(x, y)$ must be computed to about eight significant digits. This is so because of the loss of significant digits which occurs with numerical differentiation of tabular data.

Chapter 4

Chemical Transport and Fate Model

4.1 Transport and Fate Equations

This section contains basic equations for chemical and/or substrate transport and fate. The assumptions which form the basis for transport and fate model are as follows:

1. Mass transport is via advection (convection) and dispersion;
2. The x and y dispersion components are linearly dependent upon the moduli of the fluid velocity field components, i.e. for two-dimensional flow in an isotropic and homogeneous aquifer,

$$D_{xx} = \alpha_{tort} D_{L\phi} + \alpha_{dispy} \frac{(U_x)^2}{|\mathbf{U}|} + \alpha_{dispx} \frac{(U_y)^2}{|\mathbf{U}|} \quad (m^2/\text{day}) \tag{4.1}$$

and

$$D_{yy} = \alpha_{tort} D_{L\phi} + \alpha_{dispx} \frac{(U_x)^2}{|\mathbf{U}|} + \alpha_{dispy} \frac{(U_y)^2}{|\mathbf{U}|}, \quad (m^2/\text{day}) \tag{4.2}$$

where the magnitude of the local seepage velocity vector $\mathbf{U}$ is defined by

$$|\mathbf{U}| = \left((U_x)^2 + (U_y)^2\right)^{1/2} \tag{4.3}$$

and the "longitudinal" axis coincides with the y–axis (Konikow and Bredehoeft, 1978). The cross–axis dispersion coefficient D_{xy} is symmetrical so that $D_{yx} = D_{xy}$ and

$$D_{xy} = (\alpha_{dispy} - \alpha_{dispx}) \frac{U_x U_y}{|\mathbf{U}|}; \tag{4.4}$$

3. The porous medium can be partitioned into three distinct fractions:

   (a) weakly sorbing sand particles,

   (b) sorbing particles (clay minerals, etc.), and

   (c) strongly sorbing organic fraction,

   with the following Freundlich sorption rule assumed to hold for the porous medium

$$S \doteq (\%_{sand}\,\rho_{sand}\,K_{sand} + \%_{silt}\,\rho_{silt}\,K_{silt} + \%_{org}\,\rho_{org}\,K_{org})C\ ; \tag{4.5}$$

4. Chemical, which may be substrate, can be introduced into the aquifer with the "feed stream" at the inlet end ($y = 0$) or from constantly emitting sources in the aquifer; fluids added by these methods must be of low volumetric concentration and low flow rates (m^3/day) so that the previously established fluid flow field is not disturbed. It is assumed that density gradients, density stratification, or local change in the transport and/or fate properties of the porous medium does not occur;

5. Water containing chemicals can be introduced via fully penetrating injection wells or extracted from similar wells by pumping; and

6. Loss of chemical can occur via first–order loss processes including microbial and/or irreversible processes in both the free and sorbed phases and by radioactive decay in both phases.

Consideration of the balance of chemical mass in the REV leads to the linear two–dimensional transport and fate equation

$$\begin{aligned}
\epsilon(1 \;+\; & R)\frac{\partial C}{\partial t} = \frac{\partial}{\partial x}\left(\epsilon\, D_{xx}\,\frac{\partial C}{\partial x}\right) + \frac{\partial}{\partial y}\left(\epsilon\, D_{yy}\,\frac{\partial C}{\partial y}\right) \\
&+ \frac{\partial}{\partial x}\left(\epsilon\, D_{xy}\,\frac{\partial C}{\partial y}\right) + \frac{\partial}{\partial y}\left(\epsilon\, D_{yx}\,\frac{\partial C}{\partial x}\right) \\
&- \frac{\partial}{\partial x}(\epsilon\, U_x C) - \frac{\partial}{\partial y}(\epsilon\, U_y C) \\
&- \epsilon\,(\lambda_{met} + \lambda_{irr} + \lambda_{rad} + R\,(\lambda^s_{met} + \lambda^s_{rad}))C + Q_{so} \\
&+ Q_{inj}\,C_s - \frac{Q_{out}}{\rho_w}\,C,
\end{aligned} \tag{4.6}$$

where

$$R = \left(\frac{1-\epsilon}{\epsilon}\right)(\%_{sand}\,\rho_{sand}\,K_{sand} + \%_{silt}\,\rho_{silt}\,K_{silt} + \%_{org}\,\rho_{org}\,K_{org}) \tag{4.7}$$

is frequently called the retention coefficient (dimensionless) in the gas chromatography literature, while defining $R_d = 1 + R$ results in the retardation coefficient in the soil science literature. Since

$$\frac{\partial(\epsilon U_x)}{\partial x} + \frac{\partial(\epsilon U_y)}{\partial y} = \frac{(Q_{inj} - Q_{out})}{\rho_w}\ ,$$

from equation 3.3, we have upon substitution into equation 4.6,

$$\begin{aligned}\epsilon(1 \;+\; R)\frac{\partial C}{\partial t} &= \frac{\partial}{\partial x}\left(\epsilon\, D_{xx}\,\frac{\partial C}{\partial x}\right) + \frac{\partial}{\partial x}\left(\epsilon\, D_{xy}\,\frac{\partial C}{\partial y}\right) \\ &+ \frac{\partial}{\partial y}\left(\epsilon\, D_{yy}\,\frac{\partial C}{\partial y}\right) + \frac{\partial}{\partial y}\left(\epsilon\, D_{yx}\,\frac{\partial C}{\partial x}\right) \\ &- (\epsilon\, U_x)\frac{\partial C}{\partial x} - (\epsilon\, U_y)\frac{\partial C}{\partial y} - \epsilon\,\Lambda\, C + Q_{so} \\ &+ Q_{inj}\,(C_s - C/\rho_w)\,, \end{aligned} \tag{4.8}$$

where the overall first–order loss coefficient Λ is defined

$$\Lambda = \lambda_{met} + \lambda_{irr} + \lambda_{rad} + R\,(\lambda^s_{met} + \lambda^s_{rad})\,. \tag{4.9}$$

Even though equation 4.7 is linear and $\mathcal{D}_{ij}$ is a simple rectangular domain, the fact that U_x, U_y, D_{xx}, and D_{xy} can all vary quite widely over $\mathcal{D}_{ij}$ has made it impossible to obtain closed–form solutions except for the case of constant coefficients with $\alpha_{dispx} = \alpha_{dispy}$. Analytic solutions could not be found for the following initial and boundary conditions of this problem. This made it necessary to approximate $C(x, y, t)$ by means of a type of finite difference Euler–Lagrange procedure (Cheng et al. , 1984), which is a type of characteristics method.

In anticipation of this Euler–Lagrange solution procedure, the advection terms are brought to the left-hand side of equation 4.6 and the expression is multiplied by the factor $1/(\epsilon(1 + R))$ to obtain

$$\begin{aligned}\frac{\partial C}{\partial t} \;+\; U^*_x\,\frac{\partial C}{\partial x} + U^*_y\,\frac{\partial C}{\partial y} + \Lambda^* C \\ \frac{\partial}{\partial x}\left(D^*_{xx}\,\frac{\partial C}{\partial x}\right) + \frac{\partial}{\partial y}\left(D^*_{yy}\,\frac{\partial C}{\partial y}\right) + \frac{\partial}{\partial y}\left(D^*_{yx}\,\frac{\partial C}{\partial x}\right) \\ \frac{\partial}{\partial x}\left(D^*_{xy}\,\frac{\partial C}{\partial y}\right) + \frac{Q^*_{so}}{\epsilon} + \frac{Q^*_{inj}}{\epsilon}\,(C_s - C/\rho_w)\,, \end{aligned} \tag{4.10}$$

where the "effective" transport and fate coefficients are defined

$$U^*_x = \frac{U_x}{1+R}\,, \qquad U^*_y = \frac{U_y}{1+R}\,, \tag{4.11}$$

$$\Lambda^* = \frac{\Lambda}{1+R}\,, \tag{4.12}$$

$$D^*_{xx} = \frac{D_{xx}}{1+R}\,, \qquad D^*_{xy} = \frac{D_{xy}}{1+R}\,, \qquad D^*_{yy} = \frac{D_{yy}}{1+R}\,, \tag{4.13}$$

and the "effective" source/sink mass rates are defined

$$Q^*_{so} = \frac{Q_{so}}{1+R} \tag{4.14}$$

and

$$Q^*_{inj} = \frac{Q_{inj}}{1+R} \,. \tag{4.15}$$

Since the "effective" material or total derivative dC/dt is

$$\frac{dC}{dt} = \frac{\partial C}{\partial t} + U^*_x \frac{\partial C}{\partial x} + U^*_y \frac{\partial C}{\partial y} \,, \tag{4.16}$$

we obtain

$$\begin{aligned} \frac{dC}{dt} + \Lambda^* C \;\; &= \;\; \frac{\partial}{\partial x}\left(D^*_{xx}\frac{\partial C}{\partial x}\right) + \frac{\partial}{\partial y}\left(D^*_{yy}\frac{\partial C}{\partial y}\right) + \frac{\partial}{\partial x}\left(D^*_{xy}\frac{\partial C}{\partial y}\right) \\ &+ \;\; \frac{\partial}{\partial y}\left(D^*_{yx}\frac{\partial C}{\partial x}\right) + \frac{Q^*_{so}}{\epsilon} + \frac{Q^*_{inj}}{\epsilon}\left(C_s - C/\rho_w\right) \end{aligned} \tag{4.17}$$

for the transport and fate equation.

4.2 Initial Data, Boundary Data, and Total Chemical Mass

Completion of the conditions on C over the space–time cylinder $\mathcal{D} \cup (o,T)$, requires firstly that C be prescribed at time $t = 0$, i.e.,

$$C(x,y,o^+) = g(x,y) \tag{4.18}$$

(x,y) in $\mathcal{D}$ so that

$$L_w \int_{\mathcal{D}} \int C(x,y,o^+)dxdy < \infty \,. \tag{4.19}$$

Recall from Figure 3.1 that at each of the two planes $y = 0$ and $y = L_y$ the total hydraulic head is prescribed rather than the fluid fluxes. The fluid velocity field can vary across these planes, depending upon the presence or absence of injection and/or extraction wells in the interior. Conservation of chemical mass in the system is also desired. A complete accounting of all the chemical mass which enters and exits the aquifer via the inlet and exit ports is required. Simply fixing $C(x,o,t)$ and $C(x,L_y,t)$, $0 < x < L_x$, for all time $t > 0$ will not satisfy this condition (Parker and Van Genuchten, 1984). In order to satisfy the requirement, a "flux–type" concept along the inlet and exit port boundaries is introduced. This concept more closely approximates the conservation of mass than would be obtained from fixing the inlet and exit port chemical concentrations. Figures 4.1 and 4.2 show aspects of the concept of the mass conserving boundary conditions at the inlet and exit ports.

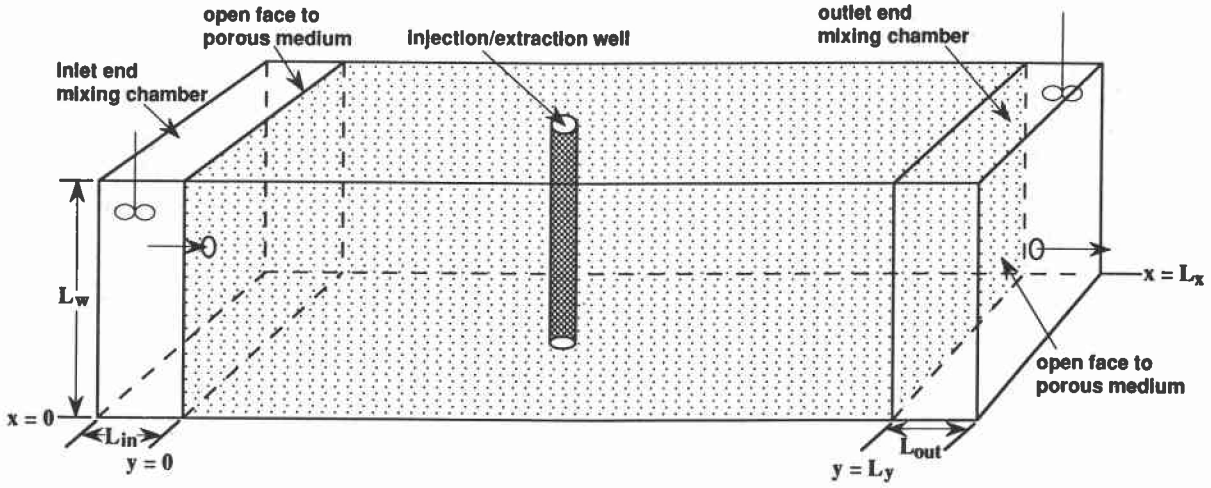

Figure 4.1: Schematic diagram of experimental arrangement used for testing the mathematical model, showing mixing chambers at inlet and outlet ends.

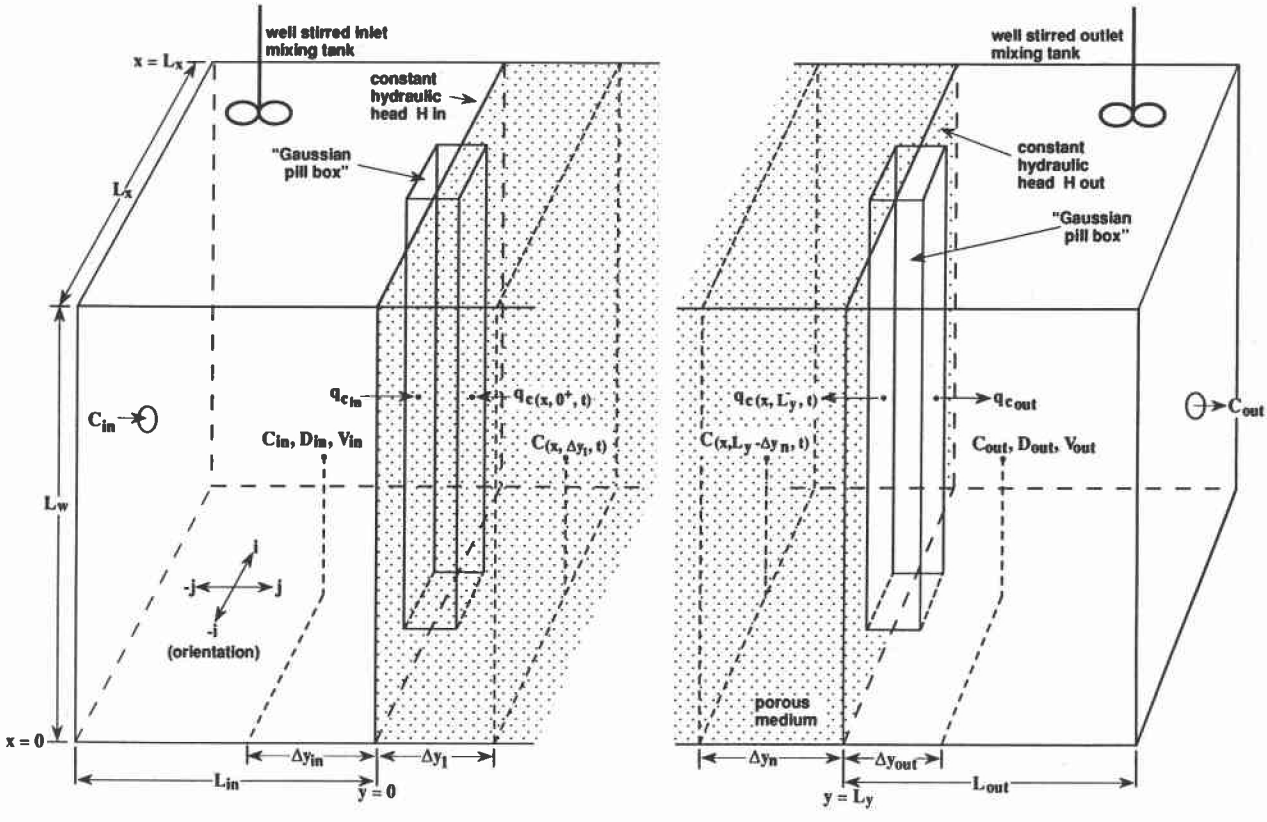

Figure 4.2: Details of the use of the "Gaussian pill box" concept in mixing chambers, flow orientation, and positions where mathematical terms were defined.

Since the chemical field flux vector can be written as

$$\mathbf{q}_c = \left(-\epsilon\, D_{xx}\,\frac{\partial C}{\partial x} - \epsilon\, D_{xy}\,\frac{\partial C}{\partial y} + \epsilon\, U_x\, C\right)\hat{\imath} + \left(-\epsilon\, D_{yx}\,\frac{\partial C}{\partial x} - \epsilon\, D_{yy}\,\frac{\partial C}{\partial y} + \epsilon\, U_y\, C\right)\hat{\jmath}\,, \qquad \left(\frac{kg}{m^2\text{–day}}\right) \tag{4.20}$$

the standard Gaussian concept of continuity in the normal component can be written for the inlet port as

$$\mathbf{q}_c|_{x,0,t} \bullet (\hat{\jmath}) + \mathbf{q}_{cin} \bullet (-\hat{\jmath}) = 0 \tag{4.21}$$

and for the exit port as

$$\mathbf{q}_c|_{x,L_y,t} \bullet (\widehat{-\jmath}) + \mathbf{q}_{cout} \bullet (\hat{\jmath}) = 0\,, \tag{4.22}$$

where the inlet port and exit port fluxes are defined by

$$\mathbf{q}_{cin} = -D_{cin}\left(\frac{C(x,0,t) - C_{in}}{\Delta y_{in}}\right) + V_{yin}\, C_{in} \tag{4.23}$$

and

$$\mathbf{q}_{cout} = -D_{cout}\left(\frac{C_{out} - C(x,L_y,t)}{\Delta y_{out}}\right) + V_{yout}\, C(x,L_y,t)\,. \tag{4.24}$$

The additional requirements for continuity of the chemical fields themselves at the bounding planes $y = 0$ and $y = L_y$ have been included in equations (4.6) and (4.8).

Since, by assumption, H is constant along the inlet and exit interfaces, $U_x \equiv 0$, making $D_{xy} = D_{yx} = 0$ as well. Therefore, along $y = 0$, we have

$$\mathbf{q}_c(x,0,t) = \left[\left(-\epsilon\, D_{xx}\frac{\partial C}{\partial x} + \epsilon\, U_x\, C\right)\hat{\imath} + \left(-\epsilon\, D_{xy}\frac{\partial C}{\partial y} + \epsilon\, U_x\, C\right)\hat{\jmath}\right]_{y=0}\,, \tag{4.25}$$

which when "dotted" with the unit normal vector $\hat{\jmath}$ obtains

$$\mathbf{q}_c(x,0,t) \bullet \hat{\jmath} = \left(-\epsilon\, D_{yy}\frac{\partial C}{\partial y} + \epsilon\, U_y\, C\right)_{y=0}\,. \tag{4.26}$$

Along $y = L_y$, we have $D_{xy} = D_{yx} = 0$ as well and

$$\mathbf{q}_c(x,L_y,t) = \left[\left(-\epsilon\, D_{xx}\frac{\partial C}{\partial x} + \epsilon\, U_x\, C\right)\hat{\imath} + \left(-\epsilon\, D_{yy}\frac{\partial C}{\partial y} + \epsilon\, U_y\, C\right)\hat{\jmath}\right]_{y=L_y}\,, \tag{4.27}$$

which when "dotted" with the unit normal vector $\widehat{-\jmath}$ obtains

$$\mathbf{q}_c(x, L_y, t) \bullet (\widehat{-j}) = \left(+\epsilon\, D_{yy} \frac{\partial C}{\partial y} - \epsilon\, U_y\, C \right)_{y=L_y} . \tag{4.28}$$

Assuming that water is an incompressible fluid, at the inlet end

$$V_{yin}(x,t) = (\epsilon\, U_y)\,|_{y=0} \,, \tag{4.29}$$

and at the outlet end

$$V_{yout}(x,t) = (\epsilon\, U_y)\,|_{y=L_y} \,. \tag{4.30}$$

Substitution of these fluxes into the two continuity equations (4.21) and (4.22) obtains

$$\begin{aligned} -D_{in} \left(\frac{C(x,0,t) - C_{in}}{\Delta y_{in}} \right) + (\epsilon\, U_y)_{y=0}\, C_{in} = & - \left(\epsilon\, D_{yy}\, \frac{\partial C}{\partial y} \right)_{y=0} . \\ & + (\epsilon\, Uy)_{y=0}\, C(x,o,t) \end{aligned} \tag{4.31}$$

for the inlet end and

$$\begin{aligned} & - \left(\epsilon\, D_{yy}\, \frac{\partial C}{\partial y} \right) \Big|_{y=L_y} + (\epsilon\, U_y)|_{y=L_y}\, C(x, L_y - \Delta y_{Ny})t) \\ & \quad = -D_{cout} \left(\frac{C_{out} - C(x, L_y, t)}{\Delta y_{out}} \right) + (\epsilon\, U_y)|_{y=L_y}\, C(x, L_y, t) \end{aligned} \tag{4.32}$$

for the outlet end conditions, respectively.

In anticipation of solving the chemical transport problem by means of a finite difference approximation, the supposition is made that

$$\frac{\partial C}{\partial y}\Big|_{y=0} \doteq \frac{C(x, \Delta y_1, t) - C(x,0,t)}{\Delta y_1} \tag{4.33}$$

and

$$\frac{\partial C}{\partial y}\Big|_{y=L_y} \doteq \frac{C(x, L_y, t) - C(x, L_y - \Delta y_{Ny}, t)}{\Delta y_{Ny}} \,. \tag{4.34}$$

Substituting these two approximations into equations (4.31) and (4.32), respectively, obtains

$$C(x,0,t) \doteq \frac{(\epsilon\, D_{yy}|_{y=0}\, \frac{C(x, \Delta y_1, t)}{\Delta y_1} + \frac{D_{cin}\, C_{in}}{\Delta y_{in}} + (\epsilon\, U_y)_{y=0}\, C_{in}}{\frac{(\epsilon\, D_{yy})_{y=0}}{\Delta y_1} + \frac{D_{cin}}{\Delta y_{in}} + (\epsilon\, U_y)_{y=0}} \tag{4.35}$$

and

$$C(x,L_y,t) \doteq \frac{\left(\epsilon\, U_y + \frac{D_{yy}}{\Delta y_{Ny}}\right)_{y=L_y} C(x, L_y - \Delta y_{Ny}, t) + \frac{D_{cout}}{\Delta y_{out}} C_{out}}{\left(\frac{\left(\epsilon U_y + \frac{\epsilon D_{yy}}{\Delta y_{Ny}}\right)_{y=L_y}}{\Delta y_{Ny}} + \frac{D_{out}}{\Delta y_{out}}\right)} \,. \tag{4.36}$$

It is easily seen from equations (4.35) and (4.36) that in the limit D_{cin} and $D_{cout} \rightarrow$ large, then $C(x,0,t) \rightarrow C_{in}$ and $C(x,L_y,t) \rightarrow C_{out}$, i.e. with the assumption of well–stirred conditions in both the inlet and outlet port mixing tanks, the diffusion gradients vanish. However, a nonzero chemical gradient may exist just inside the bounding planes $y = 0$ and $y = L_y$ in the porous medium itself.

Back substitution for $C(x,0,t)$ in the gradient portion of equation (4.6) obtains

$$\begin{aligned}(\hat{\jmath} \bullet \mathbf{q}_{cin}) &= \left(-\frac{D_{in}}{\Delta y_{in}} \left.\frac{\epsilon\, D_{yy}}{\Delta y_1}\right|_{y=0}\right) \left(\frac{C(x,\Delta y_1,t) - C_{in}}{\left.\frac{\epsilon D_{yy}}{\Delta y_1}\right|_{y=0} + \frac{D_{in}}{\Delta y_{in}} + (\epsilon\, U_y)_{y=0}}\right) \\ &+ (\epsilon\, U_y)_{y=0}\, C_{in} \,. \end{aligned} \tag{4.37}$$

Clearly, when $D_{in} \rightarrow$ large, equation (4.37) reduces to

$$(\hat{\jmath} \bullet \mathbf{q}_{cin}) = -\left.\frac{\epsilon\, D_{yy}}{\Delta y_1}\right|_{y=0} \{C(x,\Delta y_1,t) - C_{in}\} + (\epsilon\, U y)_{y=0}\, C_{in} \,. \tag{4.38}$$

If C_{in} were known, equation (4.35) could have been used as an internally consistent boundary condition. However, in most laboratory–scale aquifer situations C_{in} is not known. At best C_{in} is known indirectly, as demonstrated by the following mass balance concept.

Assuming that the constant hydraulic head boundary condition holds along the inlet face $y = 0$ and that water is incompressible, the principle of mass balance applied to the chemical mass in the well–stirred inlet tank yields

$$\frac{dM_{in}}{dt} = C_o\, L_w \int_0^{L_x} (\epsilon\, U_y)|_{y=0} dx + L_w \int_0^{L_x} (\widehat{-\jmath} \bullet \mathbf{q}_{cin}) dx \,, \tag{4.39}$$

where C_o is the constant concentration of chemical in the feed stream entering the inlet end mixing tank. Substituting for $\mathbf{q}_{cin}$ in equation (4.39), from equation (4.38) obtains

$$\begin{aligned}\frac{dM_{in}}{dt} &= C_o\, L_w \int_0^{L_x} (\epsilon\, U_y)|_{y=0} dx + L_w \int_0^{L_x} \frac{\epsilon\, D_{yy}}{\Delta y_1} C(x,\Delta y_1,t) dx \\ &- \left\{ L_w \int_0^{L_x} \left(\frac{\epsilon\, D_{yy}}{\Delta y_1} + \epsilon\, U_y\right)_{y=0} dx \right\} C_{in} \,, \end{aligned} \tag{4.40}$$

where relationship (4.29) has also been used. Since

$$M_{in} = L_x\, L_{in}\, L_w\, C_{in} \tag{4.41}$$

and L_x, L_{in}, and L_w are constant in time and space, the definition of C_{in} is obtained as the first–order differential equation,

$$\begin{aligned}\frac{dC_{in}}{dt} &= C_o \frac{1}{L_{in}L_x}\int_0^{L_x}(\epsilon\, U_y)_{y=0}dx + \frac{1}{L_{in}L_x}\int_0^{L_x}\left.\frac{\epsilon\, D_{yy}}{\Delta y_1}\right| C(x,\Delta y_1,t)dx \\ &- \left\{\frac{1}{L_{in}L_x}\left\{\int_0^{L_x}\left(\frac{\epsilon\, D_{yy}}{\Delta y_1}+\epsilon\, U_y\right)_{y=0}dx\right\}\right. C_{in}\ , \end{aligned} \tag{4.42}$$

where $C_{in}(0)$ must be specified to obtain the unique, continuous solution $C_{in}(t)$. Since, with the assumption of well–stirred inlet and outlet chambers, $C(x,0,t) = C_{in}(t)$, equation (4.42) becomes the "inlet boundary condition."

Back substituting for $C(x,L_y,t)$ in the gradient portion of equation (4.24) obtains at the outlet end

$$\begin{aligned}(\hat{j}\bullet \mathbf{q}_{cout} &= -\left.\frac{\epsilon\, D_{yy}}{\Delta y_{Ny}}\right|_{y=L_y}\left[\frac{\frac{D_{out}}{\Delta y_{out}}(C_{out}-C(x,L_y-\Delta y_{Ny},t))}{\left(\frac{\epsilon\, D_{yy}}{\Delta y_{Ny}}+\epsilon\, U_y\right)_{y=L_y}+\frac{D_{out}}{\Delta y_{out}}}\right] \\ &+ (\epsilon\, U_y)_{y=L_y}\, C(x,L_y-\Delta y_{Ny},t)\ . \end{aligned} \tag{4.43}$$

Clearly, as D_{out} becomes large in equation (4.43) we have

$$\begin{aligned}(\hat{j}\bullet \mathbf{q}_{cout} &= \left(-\left.\frac{\epsilon\, D_{yy}}{\Delta y_{N_y}}\right|_{y=L_y}(C_{out}-C(x,L_y-\Delta y_{Ny},t))\right. \\ &+ (\epsilon\, Uy)_{y=Ly}\, C(x,L_y-\Delta y_{Ny},t)\ . \end{aligned} \tag{4.44}$$

The argument for the inlet end also applies to the outlet end of the laboratory–scale aquifer.

Assuming that the constant hydraulic head boundary condition holds along the inlet face, y = 0, and that water is incompressible, applying the principle of mass balance to the chemical mass in the well-stirred outlet tank yields equation (4.45):

$$\frac{dM_{out}}{dt} = L_w\int_0^{L_x}(\hat{j}\bullet \mathbf{q}_{cout})dx - \left\{L_w\int_0^{L_x}(\epsilon\, U_y|_{y=L_y})dx\right\}C_{out}\ . \tag{4.45}$$

Substituting in this equation for q_{cout} from equation (4.44) obtains

$$\begin{aligned}\frac{dM_{out}}{dt} &= L_w\int_0^{L_x}\left[\left(\frac{\epsilon\, D_{yy}}{\Delta y_{Ny}}+\epsilon\, U_y\right)_{y=L_y}C(x,L_y-\Delta y_{Ny},t)\right]dx \\ &- -\left(L_w\int_0^{L_x}\left[\left(\frac{\epsilon\, D_{yy}}{\Delta y_{Ny}}+\epsilon\, U_y\right)_{y=L_y}dx\right]\right)dx\, C_{out}\ . \end{aligned} \tag{4.46}$$

Observe that coefficients in the integrand of equation (4.46) are equal and opposite in sign. Recall that

$$M_{out}(t) = L_{out}\, L_x\, L_w\, C_{out}(t)\ , \tag{4.47}$$

a simple first–order ordinary differential equation defining $C_{out}(t)$,

$$\frac{dC_{out}}{dt} = \frac{1}{L_{out}L_x}\int_0^{L_x}\left[\left(\frac{\epsilon\, D_{yy}}{\Delta y_{Ny}} + \epsilon\, U_y\right)_{y=L_y} C(x, L_y - \Delta y_{Ny}, t)\right] dx$$
$$- \frac{1}{L_{out}L_x}\int_0^{L_x}\left(\frac{\epsilon\, D_{yy}}{\Delta y_{Ny}} + \epsilon\, U_y\right)_{y=L_y} dx\, C_{out} \qquad (4.48)$$

is obtained. In order to solve for $C_{out}(t)$ uniquely, knowledge of $C_{out}(0)$ is required. Analogous to treatment of the inlet boundary note that

$$C(x, L_y, t) = C_{out}(t)$$

is the boundary condition on the outlet end of the aquifer. Along the planes $x = 0$ and $x = L_x$ the Neumann (no chemical flux) conditions

$$\left.\frac{\partial C}{\partial x}\right|_{x=0} = 0 = \left.\frac{\partial C}{\partial x}\right|_{x=L_x} \qquad (4.49)$$

are required. These two conditions obtain directly from applying a Gaussian pill box concept to the impervious bounding walls and recalling that $U_x = 0$, along both walls as well.

The total chemical mass in the system at time t (days) following initiation of the transport and fate processes is defined by

$$M_{Aq}(t) = L_w \int_0^{L_y}\int_0^{L_x} \epsilon(1+R)\, C(x,y,t)dxdy\,, \qquad (4.50)$$

where L_w is the vertical thickness (m) of the aquifer system.

The total cumulative chemical mass entering (+) or leaving (−) the inlet port is defined by

$$M_{\text{Inlet}}(t) = L_w \int_0^{t}\int_0^{L_x} (\mathbf{q}_c)|_{y=0} \bullet (\widehat{-j})dxd\tau\,. \qquad (4.51)$$

The total cumulative chemical mass leaving or entering (+) or leaving (−) the exit port is defined by

$$M_{\text{Outlet}}(t) = L_w \int_0^{t}\int_0^{L_x} (-\hat{j} \bullet -\mathbf{q}_c)|_{y=L_y})dxd\tau\,. \qquad (4.52)$$

The total chemical mass "lost" via all first–order processes operating in the system is defined by

$$M_{\text{Lost}}(t) = L_w \int_0^t \int_0^{L_y} \int_0^{L_x} \{\epsilon \Lambda C(x,y,\tau) + Q_{out} C/\rho_w\} dx dy d\tau \ . \tag{4.53}$$

The total cumulative chemical "gained" from distributed zero order sources, e.g. from injection wells or leaking storage tanks, is defined by

$$M_{\text{Source}}(t) = L_w \int_0^t \int_0^{L_y} \int_0^{L_x} \{Q_{SO}(x,y,\tau) + Q_{inj} C_s\} dx dy d\tau \ . \tag{4.54}$$

These five scalar mass quantities give a complete mass balance for the aquifer.

4.3 Approximate Solution for the Transport and Fate Equation

Recall the subregion in space $\mathcal{D}_{ij} \subset \mathcal{D}$, which contains the i,j^{th} nodal point of both the flow field and the chemical transport field. Partition the time coordinate $[0,T]$ into a set of adjoining time subintervals so that time $t_n = t_{n-1} + \Delta t_n$, $n = 1,2,3,\ldots N_{max}$. Define

$$\mathcal{D}^*_{ij} = \mathcal{D}_{ij} \bigcup [0,T) \tag{4.55}$$

to be a space–time subcylinder so that

$$\mathcal{D}^* = \bigcup_{i,j} \{\mathcal{D}^*_{ij}\} \tag{4.56}$$

is the global space–time cylinder. Then,

$$\mathcal{D}^*_{n,n+1} = \bigcup_{i,j} \{\mathcal{D}_{ij} \cup (t_n, t_{n+1}\} \tag{4.57}$$

is that portion of $\mathcal{D}^*$ made up of the generators of the space–time cylinder lying between the two planes $t = t_n$ and $t = t_{n+1}$. Our goal is to set up the domain for a two time level computing procedure in anticipation of choosing an explicit but conditionally stable method, such as a "forward Euler" time integrator. Figure 4.3 shows a sketch of the region of interest in $\mathcal{D}^*_{ij(n,m+1)}$.

Integration of both sides of equation (4.17) with respect to a time convolution t over $[t_n,\ t_{n+1}]$ obtains

$$C(x,y,t_{n+1}) - C(x^*_n, y^*_n, t_n) + \Lambda^* \int_{t_n}^{t_{n+1}} C(x,y,\tau) d\tau$$
$$= \int_{t_n}^{t_{n+1}} \left\{ \frac{\partial}{\partial x}\left(D^*_{xx} \frac{\partial C}{\partial x}\right) + \frac{\partial}{\partial x}\left(D^*_{xy} \frac{\partial C}{\partial y}\right) \right.$$

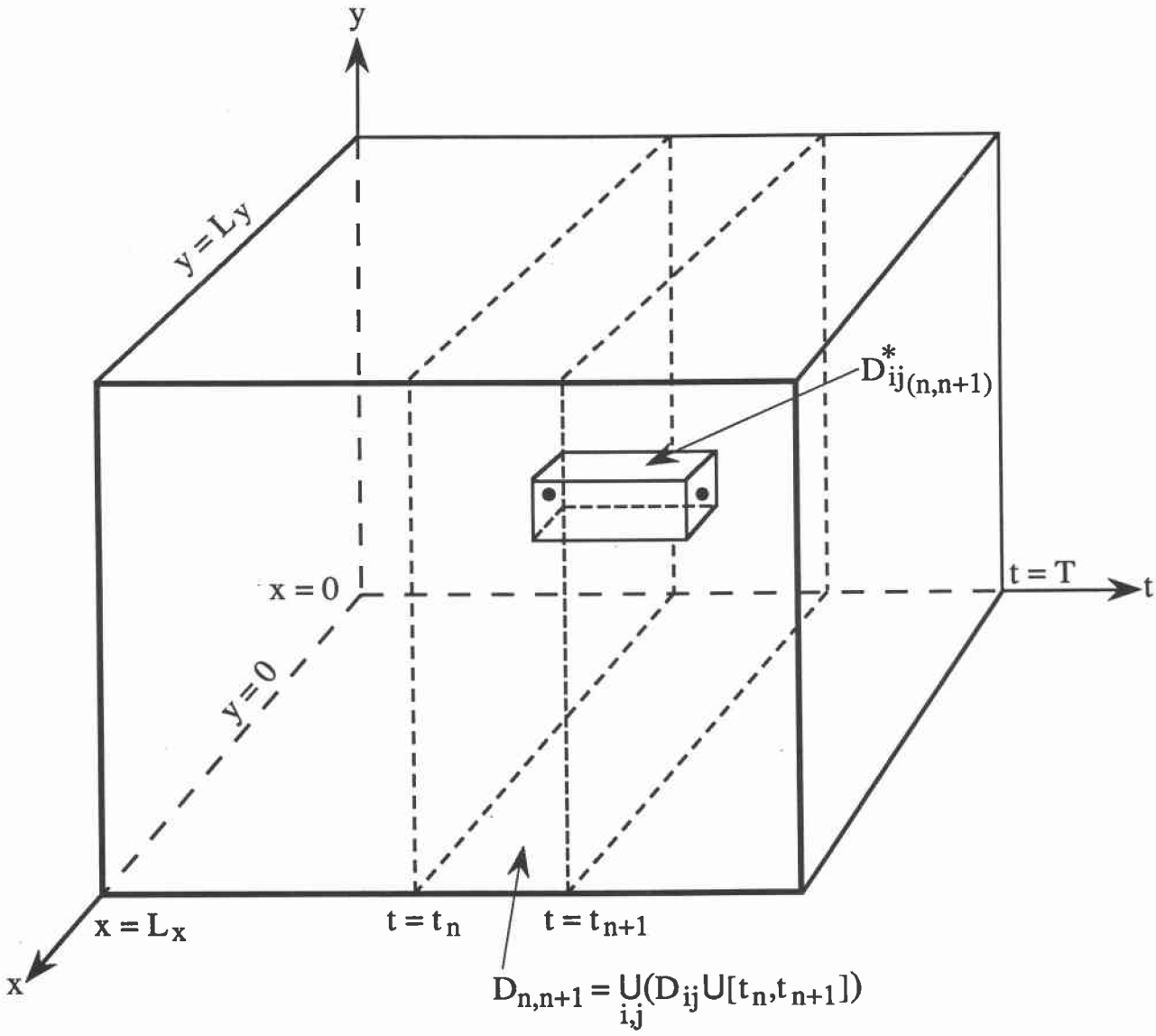

Figure 4.3: Relations among the various subregions of the overall space–time cylinder and the superimposed set of lattice points, of which one is shown at each time level.

$$+\frac{\partial}{\partial y}\left(D^*_{yx}\frac{\partial C}{\partial x}\right)+\frac{\partial}{\partial y}\left(D^*_{yy}\frac{\partial C}{\partial y}\right)\Big\}\,d\tau$$
$$+\int_{t_n}^{t_{n+1}}\left(\frac{Q^*_{so}}{\epsilon}+\frac{Q^*_{inj}}{\epsilon}\,(C_s-C/\rho_w)\right)d\tau\,, \tag{4.58}$$

where the point (x_n^*, y_n^*) is that point in $\mathcal{D}_{ij}$ at which the particle of interest resided at time level t_n and the particle moves along a material flow path connecting points (x_n^*, y_n^*) and (x_i, y_j) at time t_{n+1}. Konikow and Bredeheoft (1978) describe a method for estimating x_n^*, y_n^*, called the particle tracking method. The procedure for estimating (x_n^*, y_n^*) used here differs from the procedure of Konikow and Bredeheoft and follows more closely that of Cheng et al. (1984). A full discussion of the particle tracking method used here follows the remainder of the development of the finite difference equations by the integral method.

Next, integrate both sides of equation (4.58) over $\mathcal{D}_{ij}$ which is assumed to be stationary in time. This obtains, analogous to the spatial integration of the fluid hydraulic field equation over $\mathcal{D}_{ij}$,

$$\int_{\mathcal{D}_{ij}}\int C(x,y,t_{n+1})dxdy-\int_{\mathcal{D}_{ij}}\int C(x_n^*,y_n^*,t_n)dxdy$$
$$+\Lambda^*\int_{t_n}^{t_{n+1}}\int_{\mathcal{D}_{ij}}\int C(x,y,\tau)dxdy\,d\tau$$
$$=\int_{t_n}^{t_{n+1}}\int_{y_{j-1/2}}^{y_{j+1/2}}\left\{D^*_{xx}\left.\frac{\partial C}{\partial x}\right|_{x_{i+1/2}}-D^*_{xx}\left.\frac{\partial C}{\partial x}\right|_{x_{i-1/2}}\right.$$
$$\left.+D^*_{xy}\left.\frac{\partial C}{\partial y}\right|_{x_{i+1/2}}-D^*_{xy}\left.\frac{\partial C}{\partial y}\right|_{x_{i-1/2}}\right\}dyd\tau$$
$$+\int_{t_n}^{t_{n+1}}\int_{x_{i-1/2}}^{x_{i+1/2}}\left\{D^*_{yx}\left.\frac{\partial C}{\partial x}\right|_{y_{j+1/2}}-D^*_{yx}\left.\frac{\partial C}{\partial x}\right|_{y_{j-1/2}}\right.$$
$$\left.+D^*_{yy}\left.\frac{\partial C}{\partial y}\right|_{y_{j+1/2}}-D^*_{yy}\left.\frac{\partial C}{\partial y}\right|_{y_{j-1/2}}\right\}dxd\tau$$
$$+\int_{t_n}^{t_{n+1}}\int_{\mathcal{D}_{ij}}\int\left(\frac{Q^*_{so}}{\epsilon}+\frac{Q^*_{inj}}{\epsilon}(C_s-C/\rho_w)\right)dxdy\,d\tau\,. \tag{4.59}$$

Approximations, which have not been made so far, are now stated as follows:

1. Let

$$\tilde{C}^n_{ij}=\tilde{C}(x_i,y_j,t_n)\doteq C(x_i,y_j,t_n) \tag{4.60}$$

be the approximate distribution of the chemical field concentration, where $\tilde{C}^n_{ij}$ is defined at each lattice point of $\mathcal{D}^*$.

2. Approximate the first group of space derivatives by

$$\left.\frac{\partial C}{\partial x}\right|_{x_{i+1/2}}\doteq\frac{\tilde{C}_{i+1,j}-\tilde{C}_{i,j}}{\Delta x_i}\,, \tag{4.61}$$

$$\left.\frac{\partial C}{\partial x}\right|_{x_{i-1/2}} \doteq \frac{\tilde{C}_{i,j} - \tilde{C}_{i-1,j}}{\Delta x_{i-1}}\,, \tag{4.62}$$

$$\left.\frac{\partial C}{\partial x}\right|_{x_{i-1/2}} \doteq \frac{\tilde{C}_{i+1/2,j+1/2} - \tilde{C}_{i+1/2,j-1/2}}{\left(\frac{\Delta y_{j-1}+\Delta y_j}{2}\right)}\,, \tag{4.63}$$

$$\left.\frac{\partial C}{\partial y}\right|_{x_{i-1/2}} \doteq \frac{\tilde{C}_{i-1/2,j+1/2} - \tilde{C}_{i-1/2,j-1/2}}{\left(\frac{\Delta y_{j-1}+\Delta y_j}{2}\right)}\,. \tag{4.64}$$

The second group of first partial derivatives in equation (4.59) are approximated accordingly. Since $C_{i-1/2,j+1/2}, C_{i-1/2,j-1/2}, C_{i+1/2,j+1/2}$, and $C_{i+1/2,j-1/2}$ are chemical concentration values at points which are not lattice points of the subdomain $\mathcal{D}_{ij}$, approximate these values as follows

$$\tilde{C}_{i-1/2,j-1/2} \doteq \frac{1}{4}(\tilde{C}_{i,j} + \tilde{C}_{i-1,j-1} + \tilde{C}_{i-1,j} + \tilde{C}_{i,j-1})\,, \tag{4.65}$$

$$\tilde{C}_{i-1/2,j+1/2} \doteq \frac{1}{4}(\tilde{C}_{i,j} + \tilde{C}_{i-1,j} + \tilde{C}_{i-1,j+1} + \tilde{C}_{i,j+1})\,, \tag{4.66}$$

$$C_{i+1/2,j+1/2} \doteq \frac{1}{4}(\tilde{C}_{i,j} + \tilde{C}_{i,j+1} + \tilde{C}_{i+1,j+1} + \tilde{C}_{i+1,j})\,, \tag{4.67}$$

$$\tilde{C}_{i+1/2,j-1/2} \doteq \frac{1}{4}(\tilde{C}_{i,j} + \tilde{C}_{i,j-1} + \tilde{C}_{i+1,j+1} + \tilde{C}_{i+1,j})\,. \tag{4.68}$$

Substituting these estimates for the midpoint values shown in equations (4.63) and (4.64) as well as the two corresponding x-axis partial derivatives which are not shown, obtains

$$\left.\frac{\partial C}{\partial y}\right|_{x_{i+1/2}} \doteq \frac{\left(\frac{\tilde{C}_{i,j+1}+\tilde{C}_{i+1,j+1}}{2}\right) - \left(\frac{\tilde{C}_{i,j-1}+\tilde{C}_{i+1,j-1}}{2}\right)}{\Delta y_{j-1} + \Delta y_j}\,, \tag{4.69}$$

$$\left.\frac{\partial C}{\partial y}\right|_{x_{i-1/2}} \doteq \frac{\left(\frac{\tilde{C}_{i-1,j+1}+\tilde{C}_{i,j+1}}{2}\right) - \left(\frac{\tilde{C}_{i-1,i-1}+\tilde{C}_{i,j-1}}{2}\right)}{\Delta y_{j-1} + \Delta y_j}\,, \tag{4.70}$$

$$\left.\frac{\partial C}{\partial x}\right|_{y_{j+1/2}} \doteq \frac{\left(\frac{\tilde{C}_{i+1,j}+\tilde{C}_{i+1,j+1}}{2}\right) - \left(\frac{\tilde{C}_{i-1,j}+\tilde{C}_{i-1,j+1}}{2}\right)}{\Delta x_{i-1} + \Delta x_i}\,, \tag{4.71}$$

$$\left.\frac{\partial C}{\partial x}\right|_{y_{j-1/2}} \doteq \frac{\left(\frac{\tilde{C}_{i+1,j-1}+\tilde{C}_{i+1,j}}{2}\right) - \left(\frac{\tilde{C}_{i-1,j-1}+\tilde{C}_{i-1,j}}{2}\right)}{\Delta x_{i-1} + \Delta x_i}\,. \tag{4.72}$$

3. The effective dispersion coefficients, evaluated at the midpoints, are estimated as arithmetic means as follows:

$$D^*_{xxi+1/2,j} \doteq \frac{D^*_{xxi+1,j} + D^*_{xxi,j}}{2} , \tag{4.73}$$

$$D^*_{xxi-1/2,j} \doteq \frac{D^*_{xxi,j} + D^*_{xxi-1,j}}{2} , \tag{4.74}$$

$$D^*_{xyi+1/2,j} \doteq \frac{D^*_{xyi+1,j} + D^*_{xyi,j}}{2} , \tag{4.75}$$

$$D^*_{xyi-1/2,j} \doteq \frac{D^*_{xyi,j} + D^*_{xyi-1,j}}{2} , \tag{4.76}$$

$$D^*_{yxi,j+1/2} = D^*_{xyi,j+1/2} \doteq \frac{D^*_{xyi,j+1} + D^*_{xy,j}}{2} , \tag{4.77}$$

$$D^*_{yxi,j-1/2} = D^*_{xyi,j-1/2} \doteq \frac{D^*_{xyi,j} + D^*_{xyi,j-1}}{2} , \tag{4.78}$$

$$D^*_{yyi,j+1/2} \doteq \frac{D^*_{yyi,j+1} + D^*_{yyi,j}}{2} , \tag{4.79}$$

$$D^*_{yyi,j-1/2} \doteq \frac{D^*_{yyi,j} + D^*_{yyi,j-1}}{2} . \tag{4.80}$$

4. Q_{so} is constant over $\mathcal{D}_{ij}$ and takes on the value Q_{soij} at (x_i, y_j) for all (x, y) in $\mathcal{D}_{ij}$.

5. $$\int_{\mathcal{D}_{ij}} \int C(x,y,t)dxdy \doteq \text{Area}\,(\mathcal{D}_{ij}) \bullet \tilde{C}_{ij}(t) . \tag{4.81}$$

6. The time convolution integral for the first–order fate term is approximated at the forward–in–time point t_{n+1}, the dispersion terms are all evaluated at the backward–in–time point t_n, and the source/sink terms are evaluated at the backward–in–time point t_n.

Putting all these approximations together into equation (4.59) yields:

$$\begin{aligned}
&\text{Area}(\mathcal{D}_{ij}) \left[\tilde{C}^{n+1}_{ij} - \tilde{C}^n(P^*_{ij}) + \Lambda^* \Delta t \, \tilde{C}^n_{ij} + \Delta t \frac{Q^*_{inj_{ij}}}{\rho_w \epsilon} \tilde{C}^n_{ij} \right] \\
&= \Delta t \left(\frac{\Delta y_{j-1} + \Delta y_j}{2} \right) \left\{ \left[D^*_{xxi+1/2,j} \left(\frac{\tilde{C}^n_{i+1,j} - \tilde{C}^n_{ij}}{\Delta x_i} \right) \right. \right. \\
&\left. - D^*_{xxi-1/2,j} \left(\frac{\tilde{C}^n_{i,j} - \tilde{C}^n_{i-1,j}}{\Delta x_{i-1}} \right) \right] \\
&+ \left[D^*_{xyi+1/2,j} \left(\frac{\tilde{C}^n_{i+1/2,j+1/2} - \tilde{C}^n_{i+1/2,j-1/2}}{\frac{\Delta y_{j-1} + \Delta y_j}{2}} \right) \right.
\end{aligned}$$

$$
\begin{aligned}
&- D^*_{xyi-1/2,j}\left(\frac{\tilde{C}^n_{i-1/2,j+1/2}-\tilde{C}^n_{i-1/2,j-1/2}}{\frac{\Delta y_{j-1}+\Delta y_j}{2}}\right)\Bigg]\Bigg\} \\
&+\Delta t\left(\frac{\Delta x_{i-1}+\Delta x_i}{2}\right)\Bigg\{\Bigg[D^*_{yxi,j+1/2}\left(\frac{\tilde{C}^n_{i+1/2,j+1/2}-\tilde{C}^n_{i-1/2,j+1/2}}{\frac{\Delta x_{i-1}+\Delta x_i}{2}}\right) \\
&-D^*_{yxi,j-1/2}\left(\frac{\tilde{C}^n_{i+1/2,j-1/2}-\tilde{C}^n_{i-1/2,j-1/2}}{\frac{\Delta x_{i-1}+\Delta x_i}{2}}\right)\Bigg] \\
&+\Bigg[\left(D^*_{yyi,j+1/2}\left(\frac{\tilde{C}^n_{i,j+1}-\tilde{C}^n_{i,j}}{\Delta y_i}\right)-D^*_{yyi,j-1/2}\left(\frac{\tilde{C}^n_{i,j}-\tilde{C}^n_{i,j-1}}{\Delta y_{j-1}}\right)\right]\Bigg\} \\
&+\Delta t\left(\frac{Q^*_{so_{ij}}}{\epsilon}+\frac{Q^*_{inj_{ij}}}{\epsilon}C_s\right)\ \text{Area}(\mathcal{D}_{ij})\,, \qquad (4.82)
\end{aligned}
$$

where

$$
\text{Area}(\mathcal{D}_{ij})=\left(\frac{\Delta x_{i-1}+\Delta x_i}{2}\right)\left(\frac{\Delta y_{i-1}+\Delta y_i}{2}\right)\,,
$$

and P^*_{ij}, in $\mathcal{D}_{ij}$, is viewed as the position, at time t_n of that particle of compound which lies on the trajectory or fluid flow path, passing through (x_i, y_j) at time t_{n+1}.

We now explain how the point P^*_{ij} is found and how $C^n(P^*_{ij})$ is estimated. Figure 4.4 shows the region $\mathcal{D}_{ij}$ enclosing the point (x_i, y_j) and the eight surrounding nodes with their positions defined accordingly. Apart from the obvious situations where either U^*_x or U^*_y or both vanish identically at (x_i, y_j), U^*_x or U^*_y are signed quantities and they are assumed to be continuously differentiable functions of the space coordinates everywhere, except perhaps on top of the wells. The selection rules are defined as follows:

1. if $U^*_x \geq 0$, $U^*_y \geq 0$, P^*_{ij} lies in subregion I,
2. if $U^*_x < 0$, $U^*_y \geq 0$, P^*_{ij} lies in subregion II,
3. if $U^*_x \geq 0$, $U^*_y < 0$, P^*_{ij} lies in subregion III, and
4. if $U^*_x < 0$, $U^*_y < 0$, P^*_{ij} lies in subregion IV.

Because of the similarity in argument, only details of the estimate for position of P^*_{ij} in subregion I are shown.

Since U^*_x and U^*_y have been computed at every nodal point in $\mathcal{D}$, they are known at (x_i, y_j) and the eight surrounding nodal points, figure 4.4. Figure 4.5 shows an enlargment of region I with flow lines sketched in. The velocity components U^*_x and U^*_y are approximated with the following interpolation formulas:

$$
\tilde{U}^*_x = A^I_1 + B^I_1(x-x_i) + C^I_1(y-y_j) + D^I_1(x-x_i)(y-y_j)\,, \qquad (4.83)
$$

$$
\tilde{U}^*_y = A^I_2 + B^I_2(x-x_i) + C^I_2(y-y_j) + D^I_2(x-x_i)(y-y_j)\,, \qquad (4.84)
$$

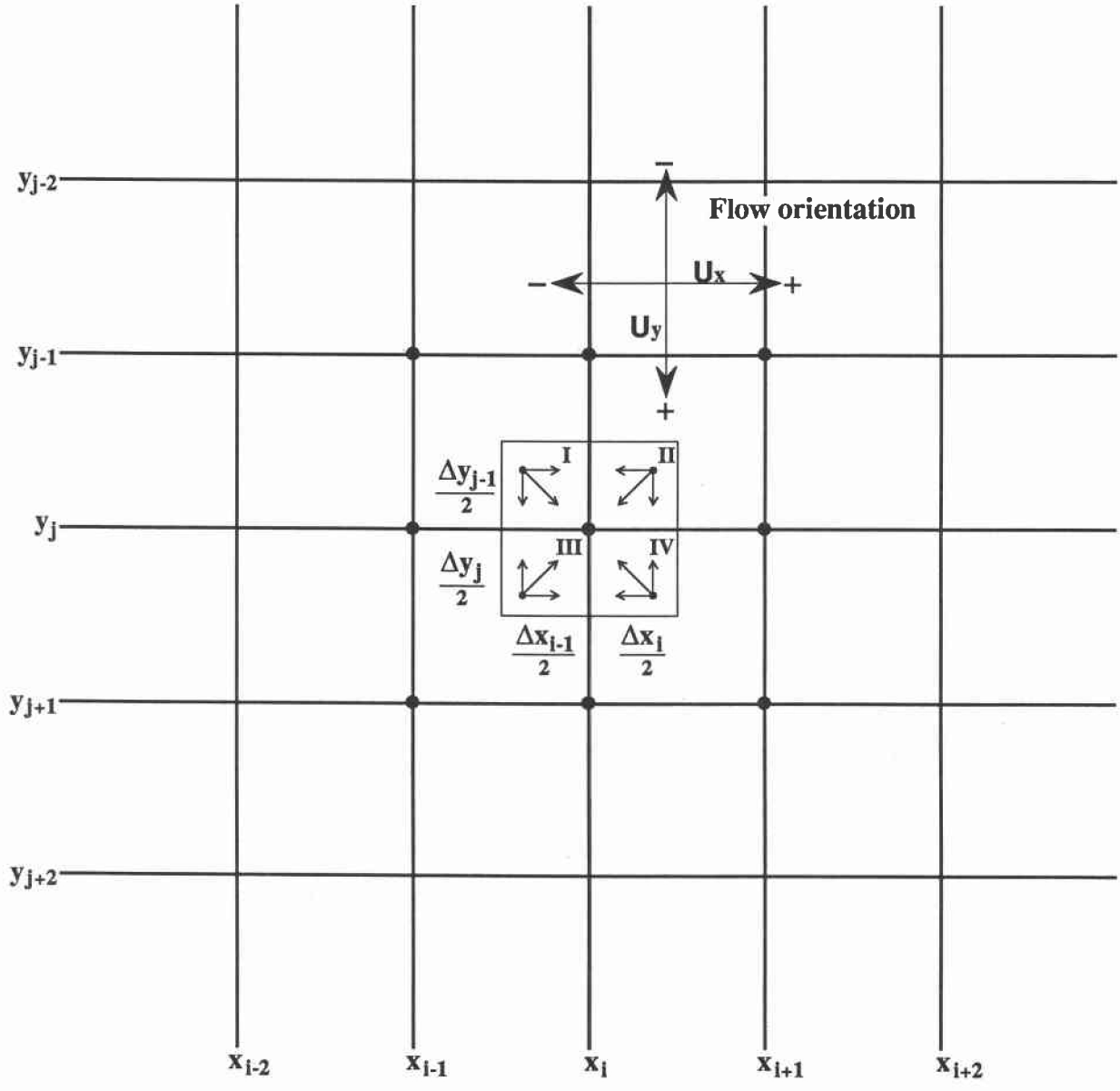

Figure 4.4: Subregion $\mathcal{D}_{ij}$ divided into four separate subregions, one of which contains P^*_{ij}. Flow orientation is also shown.

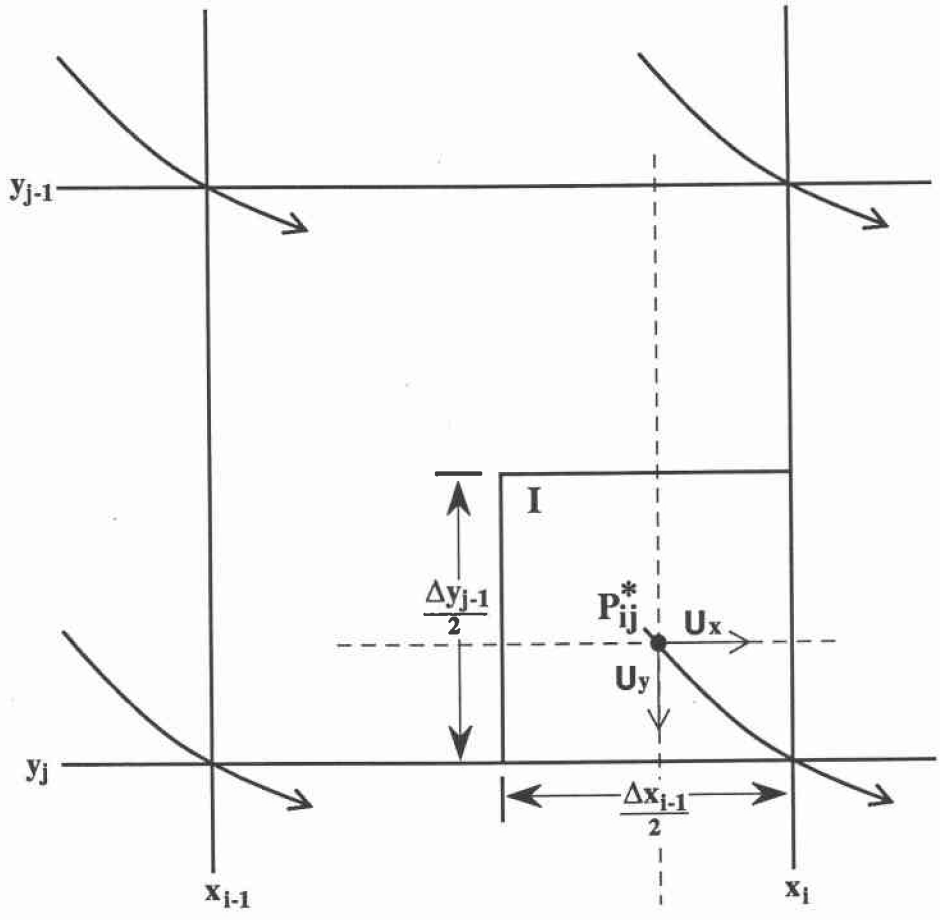

Figure 4.5: Details of procedure used to find position of point P_{ij} in region I.

where the coefficients are defined as:

$$A_1^I = U^*_{xi,j} \ , \qquad A_2^I = U^*_{yi,j} \ , \tag{4.85}$$

$$B_1^I = \frac{U^*_{xi,j} - U^*_{xi-1,j}}{\Delta x_{i-1}} \ , \qquad B_2^I = \frac{U^*_{yi,j} - U^*_{yi-1,j}}{\Delta y_{j-1}} \ , \tag{4.86}$$

$$C_1^I = \frac{U^*_{xi,j} - U^*_{xi,j-1}}{\Delta y_{j-1}} \ , \qquad C_2^I = \frac{U^*_{yi,j} - U^*_{xi,j-1}}{\Delta y_{j-1}} \ , \tag{4.87}$$

$$D_1^I = \frac{U^*_{xi,j} + U^*_{xi-1,j-1} - U^*_{xi-1,j} - U^*_{xi,j-1}}{\Delta x_{i-1} \, \Delta y_{j-1}} \ ,$$

$$D_2^I = \frac{U^*_{yi,j} + U^*_{yi-1,j-1} - U^*_{yi-1,j} - U^*_{yi,j-1}}{\Delta x_{i-1} \, \Delta y_{j-1}} \ , \tag{4.88}$$

so that both $\tilde{U}^*_x$ and $\tilde{U}^*_y$ interpolate U^*_x and U^*_y exactly at the four corner points.

Since

$$\frac{dx}{dt} = U^*_x \text{ and } \frac{dy}{dt} = U^*_y \ , \tag{4.89}$$

integrating both sides over $[t_n, t_{n+1}]$ yields

$$x(t_{n+1}) = x(t_n) + \int_{t_n}^{t_{n+1}} U^*_x \, d\tau \ , \tag{4.90}$$

$$y(t_{n+1}) = y(t_n) + \int_{t_n}^{t_{n+1}} U^*_y \, d\tau \ , \tag{4.91}$$

where now $[x(t_{n+1}), y(t_{n+1})] = (x_i, y_i)$ and $(x(t_n), y(t_n) = P^*_{ij} = (x^*_{in}, y^*_{in})$. Using a low order accuracy time quadrature approximation, which is consistent with that used in approximating the main transport and fate equation, the relationships (4.90) and (4.91) are approximated by

$$x_i \doteq x^*_i + \Delta t \, \tilde{U}^*_x \tag{4.92}$$

and

$$y_i \doteq y^*_i + \Delta t \, \tilde{U}^*_y \ , \tag{4.93}$$

where the i, j subscripts have been suppressed in the velocities. Substituting for U_x^* and U_y^* leads to the coupled system of nonlinear algebraic equations in (x_i^*, y_j^*),

$$\begin{aligned} f_1^I(x_i^*, y_j^*) &= x_i^* - x_i + \Delta t(A_1^I + B_1^I(x_i^* - x_i) + C_1^I(y_j^* - y_j) \\ &+ D_1^I(x_i^* - x_i)(y_j^* - y_j)) = 0 \end{aligned} \tag{4.94}$$

and

$$\begin{aligned} f_2^I(x_i^*, y_j^*) &= y_j^* - y_j + \Delta t(A_2^I + B_2^I(x_i^* - x_i) + C_2^I(y_j^* - y_j) \\ &+ D_2^I(x_i^* - x_i)(y_j^* - y_j)) = 0 \,. \end{aligned} \tag{4.95}$$

The classical method of Newton–Raphson–Kantorovich (Vemuri and Karplus, 1981) is then used to find (x_i^*, y_j^*) using (x_i, y_i) as the initial guess and a relative error tolerance of 10^{-4}. The theorem, which states that for all finite values of A_1^I, A_2^I, B_1^I, B_2^I, C_1^I, C_2^I, D_1^I, and D_2^I and Δt chosen,

$$\Delta t \leq \min \left[\frac{\Delta x_{i-1}}{2U_x^*}, \frac{\Delta y_{j-1}}{2U_y^*} \right] , \tag{4.96}$$

the nonlinear system equations (4.94) and (4.95) have a unique solution inside subregion I, can be proven rather easily.

With a good estimate of (x_i^*, y_j^*) now available $C^n(P_{ij}^*)$ is estimated, using the interpolation formula:

$$\begin{aligned} \tilde{C}^n(P_{ij}^*) &\doteq \alpha^I + \beta^I(x_i^* - x_i) + \gamma^I(y_j^* - y_j) \\ &+ \delta^I(x_i^* - x_i)\,(y_j^* - y_j) \,, \end{aligned} \tag{4.97}$$

where

$$\alpha^I = \tilde{C}_{i,j}^{*n} \,, \tag{4.98}$$

$$\beta^I = \frac{\tilde{C}_{i,j}^{*n} - \tilde{C}_{i-1,j}^{*n}}{\Delta x_{i-1}} \,, \tag{4.99}$$

$$\gamma^I = \frac{\tilde{C}_{i,j}^{*n} - \tilde{C}_{i,j-1}^{*n}}{\Delta y_{j-1}} \,, \tag{4.100}$$

$$\delta^I = \frac{\tilde{C}_{i,j}^{*n} + \tilde{C}_{i-1,j-1}^{*n} - \tilde{C}_{i-1,j} - \tilde{C}_{i,j-1}}{\Delta x_{i-1}\, \Delta y_{j-1}} \,. \tag{4.101}$$

Equation (4.97) produces estimates which are easily shown by standard multivariate Taylor series analysis to be $0(\Delta x_{i-1}^2 + \Delta y_{i-1}^2)$ accurate, which is in line with the low order accuracy of the approximate discrete transport and fate equation. The other three subregions yield similar formulas with the particle tracking concept being carried over from one region to

the next. The Fortran 77 encoded program LTRSKAQ2 contains the formulas for all four subregions induced about every interior nodal point.

Now divide both sides of equation (4.82) by area ($\mathcal{D}_{ij}$), substitute for the midpoint approximations for the spatial derivatives wherever indicated, and group common terms together to arrive at the explicit computing formula:

$$\begin{aligned}
\tilde{C}_{ij}^{n+1} &= alt1_{ij}\,\tilde{C}_{i-1,j-1}^{n} + alt2_{ij}\,\tilde{C}_{i-1,j}^{n} \\
&+ alt3_{ij}\,\tilde{C}_{i-1,j+1}^{n} + adt1_{ij}\,\tilde{C}_{i,j-1}^{n} + adt2_{i,j}\,\tilde{C}_{i,j}^{n} \\
&+ adt3_{ij}\,\tilde{C}_{i,j+1}^{n} + aut1_{ij}\,\tilde{C}_{i+1,j-1}^{n} + aut2_{i,j}\,\tilde{C}_{i+1,j}^{n} \\
&+ aut3_{ij}\,\tilde{C}_{i+1,j+1}^{n} + \Delta t\left(\frac{Q_{so_{ij}}}{\epsilon} + \frac{Q_{inj_{ij}}}{\epsilon}\,C_{s_{ij}}\right) \\
&+ \tilde{C}^{n}(P_{ij}^{*}) - \Delta t\left(\Lambda^{*} + \frac{Q_{inj_{ij}}}{\epsilon\,\rho_w}\,\tilde{C}_{ij}^{n}\right), \qquad (4.102)
\end{aligned}$$

where the coefficients are defined as:

$$alt1_{ij} = \Delta t\left\{\frac{(D^{*}_{xyi-1/2,j} + D^{*}_{xyi,j-1/2})/4}{\frac{(\Delta x_{i-1}+\Delta x_i)}{2}\,\frac{(\Delta y_{j-1}+\Delta y_j)}{2}}\right\}, \qquad (4.103)$$

$$alt2_{ij} = \Delta t\left\{\frac{\left(\frac{\Delta y_{j-1}+\Delta y_j}{2}\right)\frac{D^{*}_{xxi-1/2,j}}{\Delta x_{i-1}} + \frac{(D^{*}_{xyi,j-1/2} - D^{*}_{xyi,j+1/2})}{4}}{\frac{(\Delta x_{i-1}+\Delta x_i)}{2}\,\frac{(\Delta y_{j-1}+\Delta y_j)}{2}}\right\}, \qquad (4.104)$$

$$alt3_{ij} = -\Delta t\left\{\frac{(D^{*}_{xyi,j+1/2} + D^{*}_{xyi-1/2,j})/4}{\frac{(\Delta x_{i-1}+\Delta x_i)}{2}\,\frac{(\Delta y_{j-1}+\Delta y_j)}{2}}\right\}, \qquad (4.105)$$

$$adt1_{ij} = \Delta t\left\{\frac{\left(\frac{\Delta x_{i-1}+\Delta x_i}{2}\right)\frac{D^{*}_{yyi,j-1/2}}{\Delta y_{j-1}} + \frac{(D^{*}_{xyi-1/2,j} - D^{*}_{xyi+1/2,j})}{4}}{\frac{(\Delta x_{i-1}+\Delta x_i)}{2}\,\frac{(\Delta y_{j-1}+\Delta y_j)}{2}}\right\}, \qquad (4.106)$$

$$\begin{aligned}
adt2_{ij} &= -\Delta t\left\{\frac{\left(\frac{\Delta y_{j-1}+\Delta y_j}{2}\right)\left(\frac{D^{*}_{xxi+1/2,j}}{\Delta x_i} + \frac{D^{*}_{xxi-1/2,j}}{\Delta x_{i-1}}\right)}{\frac{(\Delta x_{i-1}+\Delta x_i)}{2}\,\frac{(\Delta y_{j-1}+\Delta y_j)}{2}}\right. \\
&+ \left.\frac{\left(\frac{\Delta x_{i-1}+\Delta x_i}{2}\right)\left(\frac{D^{*}_{yyi,j+1/2}}{\Delta y_j} + \frac{D^{*}_{yyi,j-1/2}}{\Delta y_{j-1}}\right)}{\frac{(\Delta x_{i-1}+\Delta x_i)}{2}\,\frac{(\Delta y_{j-1}+\Delta y_j)}{2}}\right\}, \qquad (4.107)
\end{aligned}$$

$$adt3_{ij} = \Delta t\left\{\frac{\left(\frac{\Delta x_{i-1}+\Delta x_i}{2}\right)\frac{D^{*}_{yyi,j+1/2}}{\Delta y_j} + \frac{(D^{*}_{xyi+1/2,j} - D^{*}_{xyi-1/2,j})}{4}}{\frac{(\Delta x_{i-1}+\Delta x_i)}{2}\,\frac{(\Delta y_{j-1}+\Delta y_j)}{2}}\right\}, \qquad (4.108)$$

$$aut1_{ij} = -\Delta t \left\{ \frac{(D^*_{xyi+1/2,j} + D^*_{xyi,j-1/2})/4}{\frac{(\Delta x_{i-1}+\Delta x_i)}{2}\ \frac{(\Delta y_{j-1}+\Delta y_j)}{2}} \right\}, \tag{4.109}$$

$$aut2_{ij} = \Delta t \left\{ \frac{\left(\frac{\Delta y_{j-1}+\Delta y_j}{2}\right) \frac{D^*_{xxi+1/2,j}}{\Delta x_i} + \frac{(D^*_{xyi,j+1/2} - D^*_{xyi,j-1/2})}{4}}{\frac{(\Delta x_{i-1}+\Delta x_i)}{2}\ \frac{(\Delta y_{j-1}+\Delta y_j)}{2}} \right\}, \tag{4.110}$$

$$aut3_{ij} = \Delta t \left\{ \frac{(D^*_{xyi+1/2,j} + D^*_{xyi,j+1/2})/4}{\frac{(\Delta x_{i-1}+\Delta x_i)}{2}\ \frac{(\Delta y_{j-1}+\Delta y_j)}{2}} \right\}. \tag{4.111}$$

4.4 Chemical Source Concepts and Correction

One benefit of deriving the finite difference or discrete point set approximating equation to the chemical concentration field distribution [equation (4.102)] is that we observed directly the average nature of the source rate density term Q_{so} at point (x_i, y_j). Recall from Figure 3.2 that Q_{so} evaluated at nodal point (x_i, y_j) is interpreted as being constant over the region $\mathcal{D}_{ij}$. Hence, it is possible to chose several alternatives for representing small buried sources and/or larger buried sources in $\mathcal{D}$. Two such ways are discussed.

- *Alternative 1.* Alternative 1 is the easiest way to represent small diameter sources. Figure 4.6 illustrates this alternative. Place nodal point (x_i, y_j) at the center of small region $\mathcal{D}_{ij}$. The nodal points around (x_i, y_j) are closely spaced to maximize accuracy. The physical dimensions of the rectangular source are chosen to coincide with the boundary lines of region $\mathcal{D}_{ij}$, so that the well dimensions are $(\Delta x_{i-1} + \Delta x_i)/2$ by $(\Delta y_{j-1} + \Delta y_j)/2$ with nodal point (x_i, y_j) inside $\mathcal{D}_{ij}$. If the true well size is smaller than the numerical size indicated above, the source is numerically too large and must be corrected by multiplying either Q_{soij} or Q_{inij} by the area correction factor given by equation (4.112). For true well sizes exceeding the numerical size indicated above the second alternative should be used.

$$\alpha_{ij} = \left[\frac{\text{actual area of } \mathcal{D}_{ij} \text{ included in the source}}{\text{area of } \mathcal{D}_{ij}} \right]. \tag{4.112}$$

- *Alternative 2.* Alternative 2 is illustrated by Figure 4.7. Four nodal points are used to define the four plan view corners of the single isolated source. The area of the cross–hatched region shown in Figure 4.7 must coincide with the source. However, four subregions are used in setting up the coupled system of equations approximating transport and fate. When too much area is covered the source or sink rate density, each well node must be corrected by multiplying each Q_{ij} by the factor $\alpha_{ij}, 0 \leq \alpha_{ij} \leq 1$, where α_{ij} is the area quotient defined by equation (4.112). Larger sources covering many nodal points can be built up in this fashion. By keeping the spacing between nodal points small in the region of the wells, the two alternatives produce quite similar approximate chemical concentration field distributions. Q_{SOij} is found as follows:

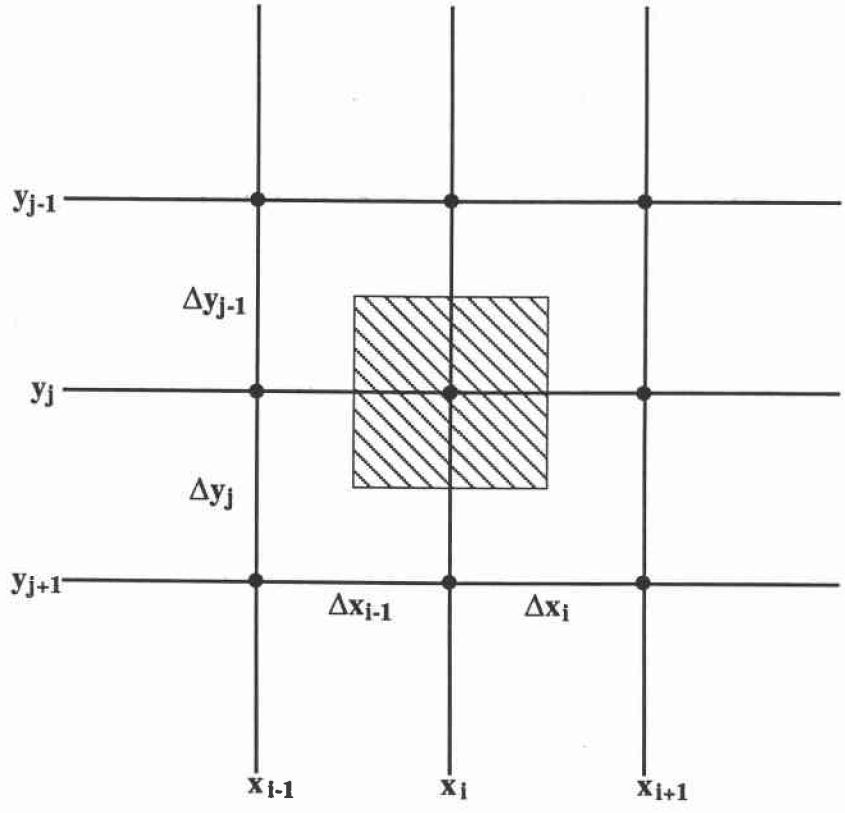

Figure 4.6: Subregion $\mathcal{D}_{ij}$ in the case of Alternative 1 for representing a single isolated source.

$$Q_{SOij} = Q_{inj_{ij}} \bullet C_{Sij} \ , \tag{4.113}$$

where $Q_{inj_{ij}}$ has the units (kg water/m^3–day) and C_{Sij}, the concentration of the substrate in the source region fluid, has the units (kg chemical/kg water) so that

$$Q_{SOij} = \left(\frac{kg \text{ water}}{m^3\text{–day}}\right)\left(\frac{kg \text{ chemical}}{kg \text{ water}}\right) = \left(\frac{kg \text{ chemical}}{m^3\text{–day}}\right) \ .$$

4.5 Boundary Conditions for Approximate Concentration Field

To complete the description of the approximate chemical concentration distribution field, $\tilde{C}^n_{ij}$, the initial and boundary data must be specified.

4.5.1 Initial data

At time $t = 0$ days define

$$\tilde{C}^o_{ij} = C(x_i, y_j\ 0^+) \ , \tag{4.114}$$

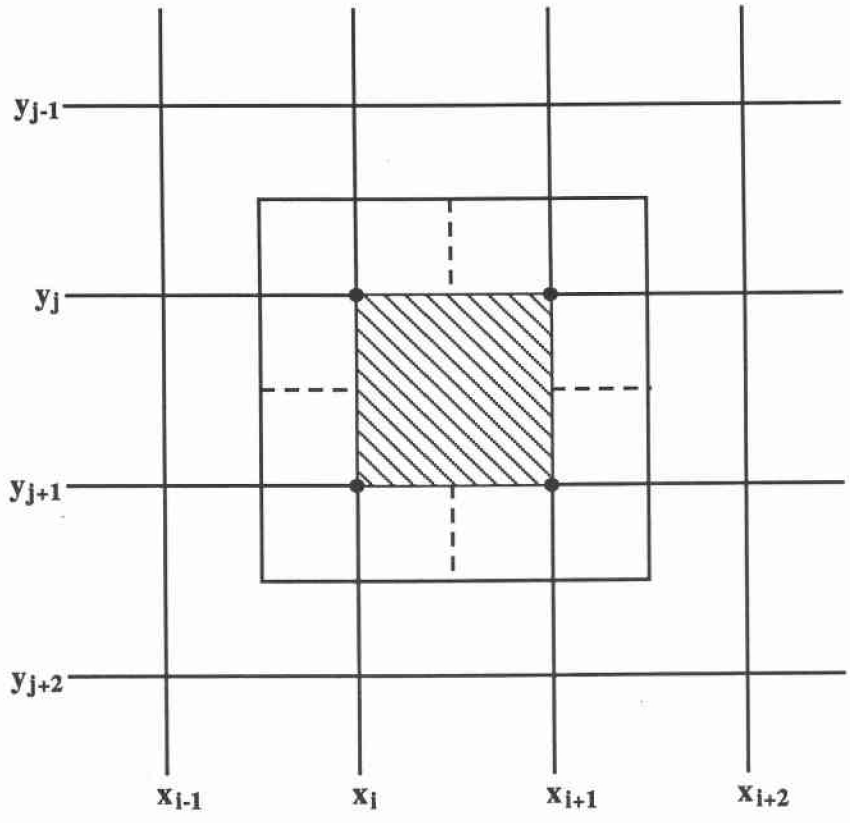

Figure 4.7: Four subregions in the case of Alternative 2 for representing a single isolated source.

which complete specifies the initial data. Recalling the geometric interpretation of C^{o}_{ij}, this means that over each region $\mathcal{D}_{ij}$ and time $t = 0$, the discrete approximation begins with the concentration being constant in the space–time cylinder, with that value of the true concentration distribution evaluated at nodal point (x_i, y_j).

4.5.2 Data at inlet and outlet ends

Recalling the definition of the inlet boundary concentration, $C_{in}(t)$, via equation (4.42), define the constants and function

$$U_{in1} = \frac{1}{L_x} \int_0^{L_x} (\epsilon\, U_y)_{y=0} dx \,, \tag{4.115}$$

$$U_{in2} = \frac{1}{L_x} \int_0^{L_x} \left(\epsilon \frac{D_{yy}}{\Delta y_1} + \epsilon\, U_y \right)_{y=0} dx \,, \tag{4.116}$$

and

$$U_{in3}(t) = \frac{1}{L_x} \int_0^{L_x} \left(\epsilon \frac{D_{yy}}{\Delta y_1} \right)_{y=0} C(x, \Delta y_1, t) dx \tag{4.117}$$

so that the differential equation defining $C_{in}(t)$ becomes

$$\frac{dC_{in}}{dt} = C_o \frac{U_{in1}}{L_{in}} + \frac{U_{in3}(t)}{L_{in}} - \frac{U_{in2}}{L_{in}} C_{in} \,. \tag{4.118}$$

This linear, first–order, Bernoulli class ordinary differential equation can be shown to have the unique time convolution solution

$$\begin{aligned} & e^{\frac{U_{in2}}{L_{in}} t_{n+1}} C_{in}(t_{n+1}) - e^{\frac{U_{in2}}{L_{in}} t_n} C_{in}(t_n) \\ & \quad = \int_{t_n}^{t_{n+1}} \left(C_o \frac{U_{in1}}{L_{in}} + \frac{U_{in3}(t)}{L_{in}} \right) e^{\frac{U_{in2}}{L_{in}} t} dt \end{aligned} \tag{4.119}$$

between the two time levels t_n and t_{n+1}. Assuming that over $[t_n, t_{n+1}]$, $U_{in3}(t)$ is continuous and one–signed, together with the known continuity and differentiability of $e^{\frac{U_{in2}}{L_{in}} t}$, apply the mean value theorem for integrals to the integral in equation (4.119). This yields, upon subsequently multiplying through both sides by $e^{-\frac{U_{in2}}{L_{in}} t}$, the formula

$$\begin{aligned} C_{in}(t_{n+1}) &= e^{-\frac{U_{in2}}{L_{in}} \Delta t} C_{in}(t_n) \\ &\quad + \frac{[C_o\, U_{in1} + U_{in3}\,(\zeta_n]}{U_{in2}} \left(1 - e^{-\frac{U_{in2}}{L_{in}} \Delta t} \right) \,, \end{aligned} \tag{4.120}$$

where ζ_n is some value of time t in $[t_n, t_{n+1}]$. Since ζ_n is not known, its value is approximated by setting $\zeta_n = t_n$, thereby making equation (4.120) an explicit time formula, which

is in line with the explicit computing formula for the approximate free–phase chemical concentration distribution, equation (4.102). The formula actually encoded is then based upon the recursive scheme

$$\begin{aligned} \chi_{in}^{n+1} &= e^{-\frac{U_{in_2}}{L_{in}}\Delta t}\,\chi_{in}^{n} \\ &+ \frac{[C_o\,U_{in1} + U_{in3}\,(t_n)]}{U_{in2}}\left(1 - e^{-\frac{U_{in2}}{L_{in}}\Delta t}\right), \end{aligned} \tag{4.121}$$

where χ_{in}^{n} is the approximation to C_{in} at time t_n. The initial condition required to get this recursive scheme going is $\chi_{in}^{0} = C_{in}^{0}$, where the zero argument of C_{in} stands for the zero point in time.

Since we do not know $U_y(x,0)$ except at each nodal point, we approximate each of the three integrals, stated in equations (4.115)– (4.117), by the classical trapezoidal rule. That is,

$$\int_0^{L_x} (\epsilon\,U_y)_{y=0} dx = \sum_{k=1}^{N_x-1} I_{1K}^{in}\,, \tag{4.122}$$

where

$$I_{1K}^{in} = \frac{\Delta x_k}{2}[\epsilon\,U_y(x_k,0) + \epsilon\,U_y(x_{k+1},0)]\,, \tag{4.123}$$

and

$$\int_0^{L_x} \left(\epsilon\,\frac{D_{yy}}{\Delta y_1} + \epsilon\,U_y\right)_{y=0} dx \doteq \sum_{k=1}^{N_x-1} I_{2K}^{in}\,, \tag{4.124}$$

where

$$I_{2K}^{in} = \frac{\Delta x_k}{2}\left[\left(\frac{\epsilon\,D_{yy}}{\Delta y_1} + \epsilon\,U_y\right)_{(x_k,0)} + \left(\frac{\epsilon\,D_{yy}}{\Delta y_1} + \epsilon\,U_y\right)_{(x_{k+1},0)}\right], \tag{4.125}$$

and

$$\int_0^{L_x} \left(\frac{\epsilon\,D_{yy}}{\Delta y_1}\right)_{y=0} C(x,\Delta y_1,t)dx \doteq \sum_{k=1}^{N_x-1} I_{3K}^{in}\,, \tag{4.126}$$

where

$$\begin{aligned} I_{3K}^{in} = \frac{\Delta x_k}{2}\Bigg(&\left.\frac{\epsilon\,D_{yy}}{\Delta y_1}\right|_{x_k,0} C(x_k,\Delta y_1,t) \\ &+ \left.\frac{\epsilon\,D_{yy}}{\Delta y_1}\right|_{x_{k+1},0} C(x_{k+1},\Delta y_1,t)\Bigg)\,. \end{aligned} \tag{4.127}$$

U_{in1} and U_{in2} are calculated only once in time, but U_{in3} must be recalculated at every time step. For the exit end tank and/or boundary condition, use equation (4.48) to define the constant and the function

$$U_{out_1} = \frac{1}{L_x} \int_0^{L_x} \left(\frac{\epsilon D_{yy}}{\Delta y_{Ny}}\bigg|_{y=L_y} + (\epsilon U_y) \right)_{y=L_y} dx \tag{4.128}$$

and

$$U_{out_2} = \frac{1}{L_x} \int_0^{L_x} \left(\frac{\epsilon D_{yy}}{\Delta y_{Ny}}\bigg|_{y=L_y} + (\epsilon U_y) \right)_{y=L_y} C(x, Ly - \Delta y_{Ny}, t) dx \ , \tag{4.129}$$

so that the differential equation defining $C_{out}(t)$ becomes

$$\frac{dC_{out}}{dt} = -\frac{U_{out1}}{L_{out}} C_{out} + \frac{U_{out2}(t)}{L_{out}} \ . \tag{4.130}$$

This first–order Bernoulli ordinary differential equation (ODE) can be treated in the same way as the ODE for the inlet tank. Over the two time–level interval $[t_n, t_{n+1}]$,

$$\begin{aligned} & e^{\frac{U_{out1}}{L_{out}} t_{n+1}} C_{out}(t_{n+1}) - e^{\frac{U_{out1}}{L_{out}} t_n} C_{out}(t_n) \\ & \quad = \int_{t_n}^{t_{n+1}} \frac{U_{out2}(t)}{L_{out}} e^{\frac{U_{out1} t}{L_{out}}} dt \ . \end{aligned} \tag{4.131}$$

Applying the mean value theorem again obtains, upon subsequently multiplying through both sides by $exp\left(-\frac{U_{out_1} t_{n+1}}{L_{out}}\right)$,

$$\begin{aligned} C_{out}(t_{n+1}) &= e^{-\frac{U_{out1}}{L_{out}} \Delta t} C_{out}(t_n) \\ &+ \frac{U_{out2}(\eta_n)}{U_{out1}} \left(1 - e^{-\frac{U_{out1} \Delta t}{L_{out}}}\right) \ , \end{aligned} \tag{4.132}$$

where η_n is a time point in the interval $[t_n, t_{n+1}]$. As before, we choose $\eta_n = t_n$ to generate an explicit formula, approximating $C_{out}(t_{n+1})$ by

$$\begin{aligned} \chi_{out}^{n+1} &= e^{-\frac{U_{out1}}{L_{out}} \Delta t} \chi_{out}^n \\ &+ \frac{U_{out2}(t_n)}{U_{out1}} \left(1 - e^{-\frac{U_{out1}}{L_{out}} \Delta t}\right) \ . \end{aligned} \tag{4.133}$$

Initially set χ_{out}^0 and apply equation (4.133) recursively in conjunction with the evaluation of $U_{out2}(t_n)$.

As was done in the case of the inlet boundary, approximate

$$\int_0^{L_x} \left(\frac{\epsilon D_{yy}}{\Delta y_{Ny}} + (\epsilon U_y) \right)_{y=L_y} dx = \sum_{k=1}^{N_x - 1} I_{1k}^{out} \ , \tag{4.134}$$

where

$$I_{1k}^{out} = \frac{\Delta x_k}{2}\left\{\left(\frac{\epsilon D_{yy}}{vy_{Ny}} + (\epsilon U_y)\Big|_{(x_i,L_y)}\right.\right.$$
$$\left.\left. + \left(\frac{\epsilon D_{yy}|}{\Delta y_{Ny}} + (\epsilon U_y)\right)\Big|_{(x_{i+1},L_y)}\right\} \tag{4.135}$$

and

$$\int_0^{L_x}\left(\frac{\epsilon D_{yy}}{\Delta y_{Ny}} + (\epsilon U_y)\Big|_{y=L_y} C(x, L_y - \Delta y_{Ny}, t)dx \doteq \sum_{k=1}^{N_x-1} I_{2k}^{out}(t)\,, \tag{4.136}$$

where

$$I_{2k}^{out}(t) = \left\{\frac{\Delta x_k}{2}\left(\left(\frac{\epsilon D_{yy}}{\Delta y_{Ny}} + (\epsilon U)\right)\Big|_{(x_i,L_y)} C(x_i, L_y - \Delta y_{Ny}, t)\right.\right.$$
$$\left.\left. + \left(\frac{\epsilon D_{yy}}{\Delta y_{Ny}} + (\epsilon U_y)\right)\Big|_{(x_{i+1},L_y)} C(x_{i+1}, L_y - \Delta y_{Ny}, t)\right)\right\}\,. \tag{4.137}$$

while U_{out1} is a constant and calculated a priori with respect to time, U_{out2} is time dependent and must be recalculated at each time step.

4.5.3 Zero flux walls

The conditions of zero chemical flux boundaries at $x = 0$ and $x = Lx$ follow naturally from equations (3.6) and (3.7):

$$\tilde{C}_{0,j}^n = \frac{\left(2 + \frac{\Delta x_2}{\Delta x_1} + \frac{\Delta x_1}{\Delta x_2}\right)\tilde{C}_{1,j}^n - \frac{\Delta x_1}{\Delta x_2}\tilde{C}_{2,j}^n}{2 + \frac{\Delta x_2}{\Delta x_1}} \tag{4.138}$$

and

$$\tilde{C}_{Nx,j}^n = \frac{-\frac{\Delta x_{Nx}}{\Delta x_{N_x-1}}\tilde{C}_{N_x-2,j}^n + \left(2 + \frac{\Delta x_{Nx}}{\Delta x_{N_x-1}} + \frac{\Delta x_{N_x-1}}{\Delta x_{Nx}}\right)\tilde{C}_{i,N_x-1,j}^n}{2 + \frac{\Delta x_{N_x-1}}{\Delta x_{Nx}}} \tag{4.139}$$

for $j = 1, 2, \ldots\ N_y - 1$.

4.6 Stability Consideration

Since the computing scheme defined by equation (4.102) is explicit, an additional stability criterion arises. Many investigators, for example Richtmyer and Morton (1967), Varga (1962), and Reddell and Sunada (1970), have considered that by choosing

$$\Delta t \leq \frac{0.5}{\max\limits_{i,j}\left(\frac{D^*_{xxij}}{\Delta x_i^2}+\frac{D^*_{yyij}}{\Delta y_j^2}\right)} \tag{4.140}$$

the computing scheme will be stable. However, Cheng et al. (1984) claim that a sufficient condition for stability is

$$\Delta t \leq \frac{1}{\max\limits_{i,j}\left(\frac{|U^*_{xij}|}{\Delta x_i}+\frac{|U^*_{yij}|}{\Delta y_j}+2\left(\frac{D^*_{xxij}}{\Delta x_i^2}+\frac{D^*_{yyij}}{\Delta y_j^2}\right)\right)}, \tag{4.141}$$

which is a tighter restriction than that given by equation (4.140). Because the flow field is at steady state it is a simple matter to calculate this value of Δt prior to the beginning of the chemical transport and fate computation. The Δt computed via equation (4.141) clearly covers that computed via equation (4.140). The other Δt value which must be considered is the requirement, equation (4.96), that the stream line, and the particle of interest "riding" on that stream line, going through (x_i, y_j) at time t_{n+1} must also pass through P^*_{ij} at time t_n. The addition of distributed first–order losses and the presence of any injection wells also further reduce the magnitude of Δt. These important restrictive conditions will be satisfied by choosing Δt so that

$$\Delta t \leq \frac{1}{\max\limits_{i,j}\left(\Lambda^*+\frac{Q^*_{inj_{ij}}}{\epsilon\,\rho_w}+\frac{2|U^*_{xij}|}{\Delta x_i}+\frac{2|U^*_{yij}|}{\Delta y_j}+2\left(\frac{D^*_{xxij}}{\Delta x_i^2}+\frac{D^*_{yyij}}{\Delta y_j^2}\right)\right)}. \tag{4.142}$$

Condition (4.142) is used as the stability criterion in this work.

4.7 Brief Summary Statement

In summary then, the approximate chemical concentration distribution $\tilde{C}^{n+1}_{ij}$ at time level t_{n+1} is obtained at each interior nodal point $(x_i y_j)$ as a linear combination of the advected, dispersed, first–order processed, and reversibly sorbed chemical, transported and/or operated upon during the time interval $[t_n, t_{n+1}]$, together with any new chemical added or removed via neighboring injection/extraction wells [equation (4.102)]. This distribution is subject to initial data [equation (4.114)], boundary data for the inlet end [equation (4.121)], and equation (4.133) for the outlet end and equations (4.137) and (4.138) along the walls where the no transverse flow boundary conditions apply.

Literature Cited

[1] Alexander, M. 1981. Biodegradation of chemicals of environmental concern. Science 211:132–138.

[2] Balkwill, D. L. and W. C. Ghiorse. 1985. Characterization of subsurface bacteria associated with two shallow aquifers in Oklahoma. Appl. Environ. Microbiol. 50:580–588.

[3] Barcelona, M. J. and T. G. Naymik. 1984. Dynamics of a fertilizer contaminant plume in groundwater. Environ. Sci. Technol. 18:257–261.

[4] Beccari, M., R. Passino, R. Ramadori and V. Tandoi. 1983. Kinetics of dissimilatory nitrate and nitrite reduction in the suspended growth culture. J. Water Pollut. Con. Fed. 55:58–64.

[5] Beeman, R. E. and J. M. Suflita. 1987. Microbial ecology of a shallow unconfined ground water aquifer polluted by municipal landfill leachate. Microb. Ecol. 14:39–54.

[6] Betz, V., G. Fischer and H. Gorbauch. 1983. The behavior of environmental pollutants in artificial aquifers. Fresenius Z. Anal. Chem. 315:464–474.

[7] Bodvarsson, G. 1984. Linearization techniques and surface operators in the theory of unconfined aquifers. Water Res. Res. 20:1271–1276.

[8] Borden, R. C. and P. B. Bedient. 1986. Transport of dissolved hydrocarbons influenced by oxygen–limited biodegradation. 1. Theoretical development. Water Resour. Res. 22:1973–1982.

[9] Borden, R. C., P. B. Bedient, M. D. Lee, C. H. Ward and J. T. Wilson. 1986. Transport of dissolved hydrocarbons influenced by oxygen–limited biodegradation. 2. Field application. Water Resour. Res. 22:1983–1990.

[10] Brown, R. A., R. D. Norris and G. R. Brubaker. 1985. Aquifer restoration with enhanced bioreclamation. Poll. Eng., 25–28.

[11] Canter, L. W. and R. C. Knox. 1986. Ground water pollution control. Lewis Publishers, Inc. Chelsea, Mi. 526 pp.

[12] Cheng, R. T., V. Casulli and S. N. Milford. 1984. Eulerian- Lagrangian solution of the convection–dispersion equation in natural coordinates. Water Resour. Res. 20:944–952.

[13] Devary, J. L. and T. J. McKeon. 1986. An evaluation of macro– dispersion from the bordon tracer experiment. Draft report for EPA contract No. 68–01–7290.

[14] Dodds, W. K. and R. D. Jones. 1987. Potential rates of nitrification and denitrification in an oligotrophic freshwater sediment system. Microb. Ecol. 14:91–100.

[14] Dodds, W. K. and R. D. Jones. 1987. Potential rates of nitrification and denitrification in an oligotrophic freshwater sediment system. Microb. Ecol. 14:91–100.

[15] Fairchild, D. M. 1987. Ground water quality and agricultural practices. Lewis Publishers, Inc. Chelsea, Michigan. 402 pp.

[16] Gorelick, S. M., C. I. Voss, P. E. Gill, W. Murray, M. A. Saunders and M. H. Wright. 1984. Aquifer reclamation design: The use of contaminant transport simulation combined with nonlinear programing. Water Resour. Res. 20:415–427.

[17] Kissel, J. C., P. L. McCarty and R. L. Street. 1984. Numerical simulation of mixed–culture biofilm. J. Environ. Eng. 110:393–411.

[18] Konikow, L. F. and J. D. Bredehoeft. 1978. Computer model of two- dimensional solute transport and dispersion in ground water. In: Techniques of water–resources investigations of the United States Geological Survey, Book 7, Chapter C2.

[19] Lehr, J. H and D. M. Nielsen. 1982. Aquifer restoration and ground water rehabilitation—A light at the end of the tunnel. Ground Water 20:650–656.

[20] Lowrance, R. 1987. Denitrification in groundwater from a coastal plain aquifer. Agron. Abstracts. Paper for Am. Soc. Agron. Meeting, Atlanta, Georgia, Nov. 29–Dec. 4.

[21] Molz, F. J., O. Guven and J. G. Melville. 1983. An examination of scale–dependent dispersion coefficients. Ground Water 21:715–725.

[22] Molz, F. J., M. A. Widdowson and L. D. Benefield. 1986. Simulation of microbial growth dynamics coupled to nutrient and oxygen transport in porous media. Water Resour. Res. 22:1207–1216.

[23] Naymik, T. G. 1987. Mathematical modeling of solute transport in the subsurface. CRC Critical Reviews in Environ. Control 17:229–251.

[24] Obenhuber, D. C., R. R. Lowrance and M. D. Erdman. 1987. The influence of nitrate and carbon additions on microbial numbers, biomass and biodegradation rates in groundwater microcosms. Agron. Abstracts. Paper for Am. Soc. Agron. Meeting, Atlanta, Georgia, Nov. 29–Dec. 4.

[25] Parker, J. C. and M. Th. Van Genuchten. 1984. Flux–averaged and volume–averaged concentrations in continuum approaches to solute transport. Water Resour. Res. 20:866–872.

[26] Pickens, J. F. and G. E. Grisak. 1981. Scale–dependent dispersion in a stratified granular aquifer. Water Resour. Res. 17:1191–1211.

[27] Pye, V. I., R. Patrick and J. Quarles. 1983. Groundwater contamination in the United States. Univ. Pennsylvania Press, Philadelphia. 314 pp.

[28] Reddell, D. L. and D. K. Sunada. 1970. Numerical simulation of dispersion in ground water aquifers. Colorado State Univ. Hydrology Paper No. 41. 79 pp.

[29] Richtmyer, R. D. and K. W. Morton. 1967. Difference Methods for Initial–Value Problems. Wiley Interscience Publishers, Inc., New York. 405 pp.

[30] Smith, L. and F. W. Schwartz. 1981. Mass transport. 3. Role of hydraulic conductivity data in prediction. Water Resour. Res. 17:1463–1479.

[31] Thomas, J. M., M. D. Lee, P. B. Bedient, R. C. Borden, L. W. Canter and C. H. Ward. 1987. Leaking underground storage tanks: Remediation with emphasis on

[32] van der Hoek, J. P. and A. Klapwijk. 1987. Nitrate removal from ground water. Water Res. 21:989–997.

[33] Varga, R. S. 1962. Matrix Iterative Analysis. Prentice–Hall, Englewood Cliffs, NJ. 322 pp.

[34] Vemuri, V. and W. J. Karplus. 1981. Digital Computer Treatment of Partial Differential Equations. Prentice-Hall, Englewood Cliffs, NJ. 449 pp.

[35] White, D. C., J. S. Nickles, J. H. Parker, R. H. Findlay, M. S. Gehron, G. A. Smith and R. F. Martz. 1985. Biochemical measures of the biomass, community structure, and metabolic activity of the ground water microbiota. In: Ward, C. H., W. Giger and P. L. McCarty (eds.) Ground Water Quality. John Wiley and Sons, New York. pp. 307–329.

[36] Wilson, J. T., J. F. McNabb, D. L. Balkwill and W. C. Ghiorse. 1983. Enumeration and characterization of bacteria indigenous to a shallow water– table aquifer. Ground Water 21:134–142.

[37] Yates, S. R. 1988a. An analytical solution to saturated flow in a finite stratified aquifer. Ground Water 26:199–206.

[38] Yates, S. R. 1988b. Seepage in a saturated–stratified aquifer with recharge. Soil Sci. Soc. Am. J. 52:356–363.